ELSEVIER

Journal of Archaeological Science 35 (2008) 191–212

Journal of Archaeological SCIENCE

http://www.elsevier.com/locate/jas

Geoarchaeological tsunami deposits at Palaikastro (Crete) and the Late Minoan IA eruption of Santorini

Hendrik J. Bruins [a,*], J. Alexander MacGillivray [b], Costas E. Synolakis [c,d], Chaim Benjamini [e], Jörg Keller [f], Hanan J. Kisch [e], Andreas Klügel [g], Johannes van der Plicht [h,i]

[a] *Ben-Gurion University of the Negev, Jacob Blaustein Institutes for Desert Research, Sede Boker Campus, 84990, Israel*
[b] *British School of Archaeology at Athens, Odos Souedias 52, 10676 Athens, Greece*
[c] *University of Southern California, Director, Tsunami Research Center, Viterbi School of Engineering, Los Angeles, CA, USA*
[d] *Technical University of Crete, Director, Natural Hazards Laboratory, Chania, Greece*
[e] *Ben-Gurion University of the Negev, Department of Geological and Environmental Sciences, 84105 Beer Sheva, Israel*
[f] *University of Freiburg, Institute of Mineralogy, Petrology and Geochemistry, 79104 Freiburg, Germany*
[g] *University of Bremen, Department of Geosciences, 28334 Bremen, Germany*
[h] *University of Groningen, Centre for Isotope Research, Nijenborgh, Groningen, The Netherlands*
[i] *Faculty of Archaeology, Leiden University, Leiden, The Netherlands*

Received 13 May 2007; received in revised form 23 August 2007; accepted 24 August 2007

Abstract

The explosive eruption at Santorini in the Aegean Sea during the second millennium BCE was the largest Holocene volcanic upheaval in the Eastern Mediterranean region. The eruption was disastrous for the Minoan settlements at Santorini, but the effect on human society in the neighbouring islands and regions is still clouded in uncertainty. Tsunami generation was suggested, but comparatively little evidence was found. The lack of firm tsunami traces is particularly puzzling in Crete with its coastal settlements of the Late Minoan IA period, during which the Santorini eruption occurred. Here, we report the discovery of extensive geoarchaeological tsunami deposits at Palaikastro in north-eastern Crete. These deposits are characterized by a mixture of geological materials, including volcanic Santorini ash, and archaeological settlement debris. Various tsunami signatures were identified: (1) erosional contact with the underlying strata, (2) volcanic ash intraclasts in the lower part of the deposit, (3) reworked building stone material in the lower part of the deposit, (4) individual marine shells, (5) marine micro-fauna, (6) imbrication of rounded beach pebbles, settlement debris, ceramic sherds and even bones, (7) multi-modal chaotic composition. Late Minoan human settlement activities at Palaikastro provided architectural and stratigraphic frameworks in space and time that recorded and preserved tsunami evidence as geoarchaeological deposits. Such stratigraphic resolution and preservation may not occur in the natural landscape. Volcanic ash transported by wind from Santorini south-east to Crete preceded the tsunami. Geological, archaeological and radiocarbon dating criteria all converge, indicating that the tsunami deposits are coeval with the Minoan Santorini eruption. Field evidence suggests that tsunami waves at Palaikastro were at least 9 m high. Inverse tsunami modeling was attempted, based on these newly discovered tsunamigenic deposits. The initial wave in the generation region at Santorini that best fits the stratigraphic data is a wave with +35 to −15 m initial amplitude and a crest length of about 15 km.

Keywords: Minoan Santorini eruption; Crete; Geoarchaeological tsunami deposits; Micromorphology; Volcanic ash geochemistry; Radiocarbon dating; Tsunami modeling

* Corresponding author. Tel.: +972 8 659 6863/6875 (secr.); fax: +972 8 659 6881.
E-mail address: hjbruins@bgu.ac.il (H.J. Bruins).

0305-4403/$ - see front matter © 2007 Elsevier Ltd. All rights reserved.
doi:10.1016/j.jas.2007.08.017

1. Introduction

The explosive eruption of the Santorini volcano in the Aegean Sea (Fig. 1) during the Late Minoan IA period (LM IA) is of great significance as a regional stratigraphic and chronological marker in the Eastern Mediterranean region (Bond and Sparks, 1976; Doumas, 1983; Keller et al., 1978, 1990; Sparks and Wilson, 1990; Druitt et al., 1999; Friedrich, 2000). Reassessment of the total volume of discharged tephra (McCoy and Dunn, 2002) and particularly the discovery by Sigurdsson et al. (2006) of massive pyroclastic deposits below sea level around Santorini indicate that the eruption was significantly larger than previous estimates. The Minoan Santorini eruption is now considered comparable to the 'super-colossal' Tambora eruption in Indonesia in 1815 (Sigurdsson et al., 2006), the largest volcanic eruption known in historical times (Sigurdsson and Carey, 1989), classified with a volcanic explosivity index (VEI) of 7 (maximum defined VEI = 8).

The well-known Krakatau eruption of 1883 (Simkin and Fiske, 1983), which occurred on a volcanic island in between Java and Sumatra, had a VEI of 6, *i.e.* 'colossal'. The eruption began on 20 May 1883 and volcanic activity continued for a few months until the final cataclysmic explosive events on August 26 and 27. Tsunamis were generated by emplacement of pyroclastic flow deposits, caldera collapse of the northern part of Krakatau Island and a huge submarine explosion (Nomanbhoy and Satake, 1995). The main catastrophic tsunami occurred on 27 August 1883 and caused the death of more than 36,000 people, as 295 villages and towns were destroyed or damaged in Java and Sumatra along the Sunda Strait (Simkin and Fiske, 1983). Pumice-bearing tsunami deposits of the Krakatau eruption were studied by Carey et al. (2001). The dramatic effects of the 1883 Krakatau catastrophe inspired Marinatos (1939) to suggest that widespread Late Minoan archaeological destruction levels in Crete may have been caused by the Santorini eruption, including tsunami impact along the coast.

However, subsequent research did not yield conclusive evidence to substantiate this hypothesis. The effect of the Minoan Santorini eruption on Crete (Fig. 1) is thought to have been limited in terms of the effect of volcanic ash deposition, while tsunami evidence has remained elusive (Thorarinsson, 1978; Keller, 1980a; Doumas and Papazoglou, 1980; Driessen and Macdonald, 1997, 2000; Dominey-Howes, 2004). Yet the 'super-colossal' magnitude of the eruption must have had consequences for the Aegean civilizations and their eastern Mediterranean neighbours. The decline of the Minoan civilization on Crete is thought to be related to the eruption (Driessen and Macdonald, 1997).

Various tsunami models have been developed in relation to the Minoan Santorini eruption (Yokoyama, 1978; Antonopoulos, 1992; McCoy et al., 2000; Pareschi et al., 2006). But surprisingly little robust onshore field evidence for Minoan tsunami deposits has been found so far in the Aegean specifically and the eastern Mediterranean region in general; see Dominey-Howes (2004) for a comprehensive review. Deep-sea homogenite deposits in the Ionian Sea were attributed, however, to a possible LM IA Santorini tsunami (Cita et al., 1984). The most important onshore evidence is a 3.5 m thick reworked tephra deposit along the east coast of Thera (Santorini) near Pori, discovered by McCoy and Heiken (2000). They interpreted the make-up and spatial distribution of these layers as tsunami evidence during the later stages of

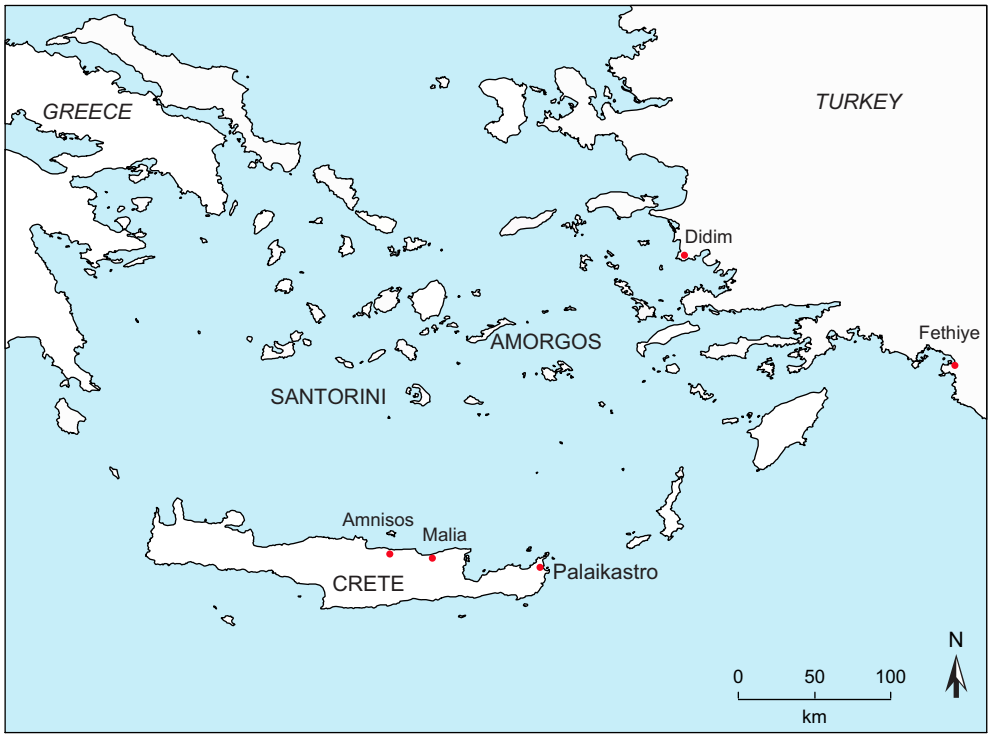

Fig. 1. Location map of the Aegean region, showing the main sites mentioned in the text.

the eruption. Other significant stratified findings are from Didim and Fethye in south-western Turkey (Fig. 1), where a *ca*. 10 cm thick sandy layer, interpreted as tsunamigenic, underlies Minoan Santorini tephra (Minoura et al., 2000).

The various phases of the LM IA Santorini eruption sequence (Bond and Sparks, 1976; Heiken and McCoy, 1984, 1990; Sparks and Wilson, 1990; McCoy and Heiken, 2000; Cioni et al., 2000) and their respective capacity for tsunami generation are summarised in Table 1. It seems unlikely that the precursor and first eruption phase (Plinian) generated tsunamis. However, pyroclastic flows that entered the sea during the second, third and fourth eruption phases might have caused tsunamis. A marine geological survey around Santorini by Sigurdsson et al. (2006) revealed the presence of massive or chaotic pyroclastic flow deposits with a mean thickness of 29 m on the ocean floor and up to 80 m thick close to the Santorini coast. Such voluminous pyroclastic flow deposits, linked by the authors to the Minoan Santorini eruption (Sigurdsson et al., 2006), may have triggered tsunamis.

Caldera collapse during the third and fourth phases also could have generated tsunamis. Important stratigraphic evidence on Thera itself, mentioned above, is thought to indicate that tsunami flooding occurred along the east coast between the third and fourth phase of the Minoan eruption (McCoy and Heiken, 2000). Moreover, Druitt et al. (1999) point out that gravel deposits, a few meters thick, overly at some locations the ignimbrite of the fourth eruption phase in a manner suggesting that the latter was still fluidized. Besides flash floods, the authors consider tsunamis generated by caldera collapse in the fourth eruption phase as a possible explanation for the gravel deposits.

1.1. Research background and rationale

Archaeological excavations in 1986 at Palaikastro in north-eastern Crete (Figs. 1–4) revealed in Building 2 (Fig. 3) evidence of initial earthquake damage, repair and finally, earthquake destruction (MacGillivray et al., 1987, pp. 150–151). This happened all during LM IA within a short time period. Possible archaeological evidence for tsunami impact was raised (MacGillivray et al., 1987, pp. 150–151). Driessen and Macdonald (1997, p. 90) suggested that the levelling of Building 2 "could just conceivably be the result of tsunami action … some time after the earthquake". However, the authors cautioned: "In searching for tsunami evidence, we are mostly clutching at straws. Further work is clearly required in this area" (Driessen and Macdonald, 1997, p. 90).

It is often difficult to detect tsunami sediments in coastal environments, as pointed out by Scheffers and Kelletat (2003). However, coastal *archaeological* sites add an extra dimension to the diagnostic potential to recognize past tsunami impact and deposition. The interaction of tsunamis with human settlements, including buildings, may leave and preserve unique geoarchaeological features. Indeed a tsunami recording mechanism is required with sufficient resolution and memory capability in space and time, which may be lacking in the natural landscape. On the other hand, past human activities in coastal settlements created stratigraphic frameworks with spatial and temporal dimensions, *i.e*. archaeological layers. Therefore, the geological impact of earthquakes and tsunamis may have been recorded and preserved in archaeological layers in coastal settlements, while leaving no decipherable traces in the more static or erosive natural landscape. The present research, initiated by Bruins and MacGillivray in 2001, gradually developed such a geoarchaeological approach at Palaikastro, Crete, in a generic way.

2. Tsunami signatures in terrestrial coastal environments

Tsunami studies used to be largely the domain of seismologists, numerical modelers, geophysicists and historians (Dawson and Shi, 2000). The identification and characterization of tsunami deposits in terms of geology, sedimentology and geomorphology is comparatively new (Dawson and Shi, 2000; Jaffe and Gelfenbaum, 2002; Scheffers and Kelletat, 2003; Scheffers, 2004; Dominey-Howes, 2004; Smith, 2005; Dominey-Howes et al., 2006). The issue is succinctly summed up by Scheffers and Kelletat (2003, p. 83): "At least 100 mega-tsunami in different parts of the world have been recorded in the past 2000 years — but presumably far more have failed to be noticed during historical times and are not mentioned either in written or oral ancient records. Therefore, the topic of paleo-tsunami requires inevitable sedimentological and geomorphological research. However, field research concerning palaeo-tsunamis is astonishingly rare within the scientific approach and only 5% of the existing tsunami literature is related to this subject".

Table 1
The phases of the LM IA Santorini eruption and their respective capacity for tsunami generation

Eruption phases	Volcanic activity	Volcanic deposition type	Maximum thickness of deposits on Santorini (m)	Tsunami generation
Precursor	Phreatic to phreatomagmatic	Ash, fine pumice and lithics	0.08	Unlikely
Phase 1	Magmatic (Plinian)	Pumice, ash, minor lithic component	7	Unlikely
Phase 2	Phreatomagmatic, incipient subsidence	Pyroclastic surge deposits with thin pumice-fall layers	12	Possible
Phase 3	Phreatomagmatic, beginning of caldera collapse	Pyroclastic flow deposits (massive), large lithic blocks	55	Likely
Phase 4	Hot pyroclastic flows, completion of caldera collapse	Ignimbrites, debris flow and co-ignimbrite ash-fall deposits	60	Likely

Sources: McCoy and Heiken (2000), Bond and Sparks (1976), Heiken and McCoy (1984, 1990), Sparks and Wilson (1990), Druitt et al. (1999), and Cioni et al. (2000).

Fig. 2. The greater Palaikastro region in eastern Crete, displaying the shape of the coast, Mount Kastri and the Mount Petsofas range; a white rectangle indicates the research area.

Tsunami inundation at the coast can be destructive and erosive, removing chunks of coastlines, as well as constructive – leaving deposits along the coast. Both types of impact were recently reported in relation to the catastrophic Sumatra tsunami in December 2004 (Liu et al., 2005; Synolakis and Kong, 2006; Jaffe et al., 2006; Moore et al., 2006; Goff et al., 2006). The effects of tsunami wave action will be very much influenced by the geomorphology of the coast and the material

Fig. 3. The research area with indicated field sections and the archaeological excavation area in the west, including the position of excavated buildings mentioned in the text.

Fig. 4. View of the research area, seen from Mount Kastri, showing the Promontory peninsula, East Beach, Chiona Beach and the archaeological excavation area.

available for deposition. A mere layer of sand is often the only trace of tsunami deposition (Minoura et al., 2000; Gelfenbaum and Jaffe, 2003; Scheffers and Kelletat, 2003; Jaffe et al., 2006; Dominey-Howes et al., 2006), but large boulders can also be deposited, if such a source is available (Scheffers, 2004).

A list of palaeo-tsunami signatures that were recognized in various deposits worldwide, compiled by Dominey-Howes (2004) and Dominey-Howes et al. (2006), include: (1) erosional contact – basal unconformity – with the underlying sediment, (2) the lower tsunami unit may contain rip-up intraclasts or reworked material or (3) basal load structures, (4) appearance of individual marine shells or mollusc rich horizons, (5) fining upwards of particles size in tsunami sediments, (6) landward fining of particles size in tsunami sediments, (7) separate tsunami waves may deposit individual layers, (8) run-up landward and backwash seaward currents may cause imbrication of shells, low-angle wedged shaped lamination or cross-bedding, (9) imbricated boulders at the coast, and (10) microfossil assemblages of diatoms and foraminifera.

Moreover, chaotic particle size composition of tsunami deposits was found to characterize various coastal areas where both fine and coarse materials are available. The minimal sorting is due to the very short time frame of the tsunami depositional processes (Dawson and Shi, 2000; Bryant, 2001; Scheffers and Kelletat, 2004). Ten main types of chaotic or bimodal tsunami sediments, all mixtures of sand and coarser debris without stratification, were recognized by Scheffers and Kelletat (2004) in the following areas: Cyprus, Mallorca, Spain, Long Island, Bahamas, Guadeloupe, Aruba, Bonaire, Curaçao, and St. Lucia.

Chaotic deposits were also caused by the 2004 Sumatra tsunami in various human settlements, consisting of smashed building debris, material cultural objects, local soil and/or beach sediments (Liu et al., 2005; Maheshwari et al., 2006). Thus it is conceivable how 'geoarchaeological tsunami signatures' – a new term introduced in this article – may be formed. Such mixtures of human settlement debris and geological materials, caused by tsunami impact, need to be differentiated from the characteristics of other archaeological formation processes (Schiffer, 1987). This is a new geoarchaeological field that has to be developed. "Tsunami evidence has rarely been proposed from archaeological sites, primarily because of a limited understanding of the requisite evidence and environmental context", as concluded by McFadgen and Goff (2007, p. 263).

3. The landscape and research area at Minoan Palaikastro

Ancient Palaikastro was one of the largest Minoan cities in Crete, but only a small part has been excavated (MacGillivray et al., 1984, 1998; Driessen and Macdonald, 1997). The landscape around the ancient Minoan town is bound in the northeast by the Aegean Sea coast and in the south by the impressive Mount Petsofas (255 m) range (Figs. 2, 4). The lithology of Mount Petsofas and the adjacent landscape includes Permian-Triassic phyllite; grey to black, massive Triassic dolomite; blue-black to grey-black, dense and thickly bedded Jurassic limestone; dark grey to black, thickly bedded Upper Cretaceous limestone; Miocene marly limestone, marl, clay, sandstone and conglomerates (Papastamatiou, 1959). Some of these rocks appear in building materials of the Minoan town and as rounded pebbles and boulders along the beach.

The Palaikastro coast forms part of a large natural bay, almost 5 km across, with small islands in the middle (Fig. 2).

Both the islands and the peninsula that closes the bay in the east have a south-west to north-east orientation, while the coastline runs from north-west to south-east (Fig. 2). Mount Kastri, an isolated table mount (90 m), composed of Miocene marly limestone, divides the coastline in two sections (Fig. 2). The Kouremenos beach stretches north-west of Mount Kastri and the beaches of Palaikastro lay to the south-east of this imposing hill.

The research area is indicated on Fig. 2 by a white rectangle, just south of Mount Kastri. The excavated part of the Minoan city at Palaikastro (MacGillivray et al., 1984, 1987, 1991, 1992, 1998) lies about 300 m from the present coastline and between 9 and 12 m above current sea level (Figs. 3, 4). The excavation area, which is partly roofed – Exc on Fig. 3 – is clearly visible in between plots with olive groves and other trees. The approximate spatial positions of excavated Buildings 2, 6 and 7, mentioned in the text, are indicated within the excavation zone (Fig. 3).

Much of the land in the area is private property and, therefore, only a small part of the Minoan town has so far been excavated. However, archaeological and magnetometer surveys indicated that the Minoan town was much larger than the excavated segment and extended even beyond the current coastline (MacGillivray et al., 1984). The sea level in the region during the second millennium BCE was apparently 1–2 m lower than at present (Sneh and Klein, 1984; Flemming and Webb, 1986; Kayan, 1988, 1991).

Our research involved volcanic ash findings discovered previously at the excavation site (MacGillivray et al., 1991, 1998). Our main fieldwork focussed at the coastal cliffs of the hillocks at the Promontory and the East Beach (Fig. 5). The small Promontory peninsula, which has a base of hard conglomerate, points as a finger north-eastward into the sea (Figs. 3–5). The Promontory divides the Palaikastro Bay into two parts: the Chiona Beach stretches northward and the East Beach southward (Figs. 3–5). Architectural elements of the Minoan town exposed by erosion along the coastal cliffs were studied previously (MacGillivray et al., 1984; Blackman, 2000). The Promontory and East Beach hillocks are somewhat more elevated than the hinterland (Figs. 4, 5). A coastal cliff is not present at Chiona beach (Fig. 4). The beaches are quite sandy, but rounded pebbles and boulders also occur. Hard consolidated rocks are exposed along the waterfront at Mount Kastri, the Promontory, part of the East Beach, and further along the coast to the south-east.

4. Findings and results – field sections

Our geoarchaeological research conducted since 2001 gradually involved quite a number of scientific disciplines. Archaeological excavations could not be undertaken at the coast, but surveys and limited sampling for microscopic studies and radiocarbon dating were possible. The many findings in different fields interacted with each other in the course of the research and shaped our evolving understanding and conclusions. Presentation of our results in relation to the respective scientific disciplines, as well as the different field sections (1–6), required quite a number of subsections. Hence we first give a brief synopsis of some main developments in the course of our research, in order to enable the reader to grasp the respective contributions and relationships of the various investigations.

Bruins and MacGillivray focused their attention in the beginning of this research on the nature and character of volcanic ash deposits exhibited in the archaeological excavations at Palaikastro (MacGillivray et al., 1991, 1998) within and near Buildings 6 and 7 (Fig. 3). Volcanic ash deposits were also found along the coastal cliff at the Promontory (Figs. 2–6), mixed with other sediments and ceramic sherds. Internally undisturbed samples of these various volcanic ash occurrences in their stratigraphic context were collected or sub-sampled for impregnation by epoxy in specialized labs to enable the making of thin sections for microscopic studies (Courty et al., 1989).

Initial results were presented by Bruins in 2002 – Minoan tephra deposition in drylands: soil micromorphology in relation to aeolian transport and post-sedimentary changes – at the Chapman Conference of the American Geophysical Union

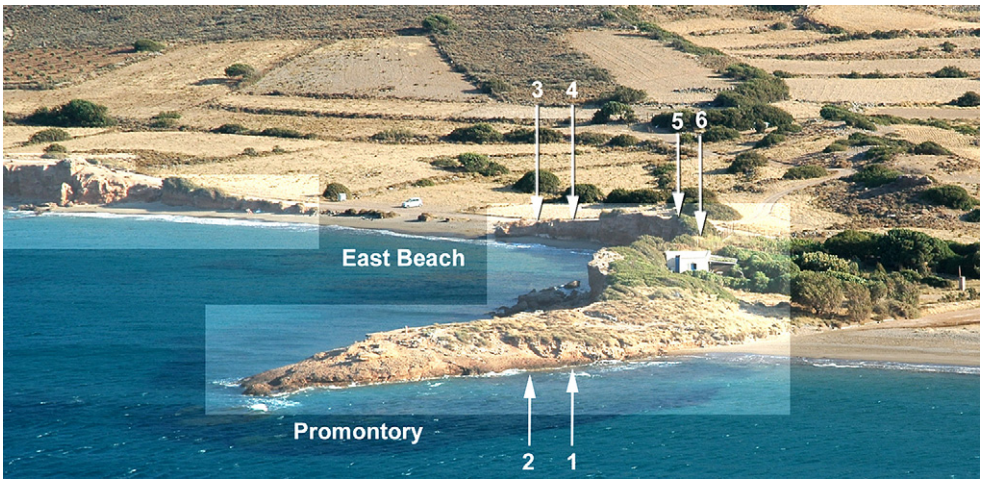

Fig. 5. The Promontory and East Beach hillocks with indicated field sections; the highlighted hillock areas are geomorphologically isolated from the hinterland, *i.e.* rainstorms cannot cause deposition on these hillocks.

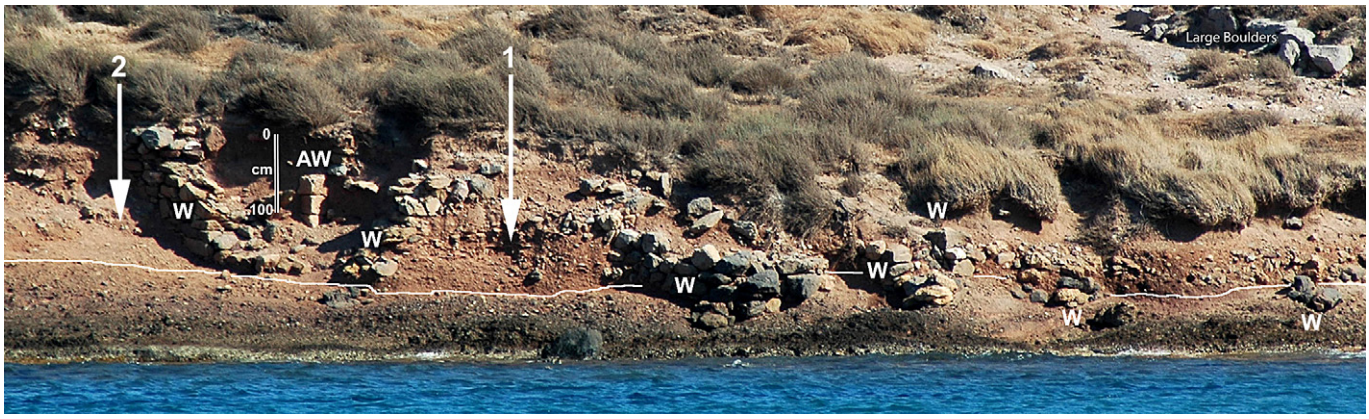

Fig. 6. The northern cliff of the Promontory peninsula in detail.

on Volcanism and the Earth's Atmosphere, held at Santorini. Though reworking and redeposition of the airborne volcanic ash in water was clear from the stratigraphy and micromorphology, no mention was made of possible tsunami relationships, considered premature at this stage of the research.

Geochemical investigations conducted by Keller (Electron Probe Micro-Analysis for major elements at the University of Freiburg) and by Klügel (Laser Ablation Inductively Coupled Plasma Mass Spectrometry for trace elements at the University of Bremen) proved unequivocally that the LM IA Santorini eruption is the source of all volcanic ash finds at Palaikastro mentioned in this paper.

A marine shell (*Patellidae*) was found *in situ* by Bruins in 2001 at the Promontory next to volcanic Santorini ash and ceramic sherds (Fig. 9). Radiocarbon dating of this marine shell by Van der Plicht at the University of Groningen yielded a ^{14}C result coeval in radiocarbon years with the LM IA Santorini eruption. This result was very important in the course of our research, as it strengthened the hypothesis of tsunami inundation in the Minoan town of Palaikastro at the time of the Santorini eruption.

Geomorphological and geoarchaeological field investigations by Bruins and MacGillivray at the coastal Promontory and East Beach hillocks continued, also in cooperation with Synolakis in the framework of the Aegean Tsunamis Research Programme. More and more sedimentary features were noted at the coastal cliffs that match tsunami signatures. Thin sections were studied by microscope at the Ben-Gurion University, concerning the micromorphology of the sediments (Bruins), petrology (Kisch) and the presence of marine micro-fauna (Benjamini). Finally, the accumulative field evidence of tsunami deposits was used for inverse tsunami modeling (Synolakis). Methodological details are presented below in relation to the results of each disciplinary research element.

4.1. Promontory and East Beach cliffs

Careful observations of the geomorphology and sedimentary stratigraphic features along the coastal cliffs along the Promontory and East Beach yielded significant discoveries of tsunami signatures, detailed below. It is important to realize that the Promontory and East Beach hillocks rise to *ca.* 8 m above sea level, but are isolated from the hinterland and the steep Mount Petsofas range by a gentle valley (Fig. 5). Therefore, stream or runoff flows coming from the hinterland and Mount Petsofas catchment area *cannot* cause deposition on the Promontory and East Beach hillocks. Hence the sedimentary features found within the geoarchaeological layers exposed at the cliffs have to be explained by other mechanisms, leaving movement by seawater as the only feasible alternative.

The position of wall remains of Minoan buildings at the very edge of the Promontory and East Beach cliffs (MacGillivray et al., 1984) indicate that the hillocks were larger in area and extended more seaward during Minoan times. A cluster of very large boulders on top of the Promontory along the path that leads southward to the beginning of the East Beach cliff (Fig. 6, upper right corner) were part of an ancient building. The erosion of the cliff face is still continuing at present and chunks of sediment slide occasionally into the water along the steep and high part of the East Beach. Six sections along the coastal cliff with distinct features were selected (Fig. 5) and are presented in the following subsections.

4.2. Promontory: field section 1

The base of the coastal cliff along the northern side of the Promontory is formed by a hard conglomerate. Eight remains of walls, apparently founded on the conglomerate, are visible (Fig. 6). The highest quality wall remnant is composed of three dressed stones – ashlars – (AW on Fig. 6), each about 23–25 cm high. Two prominent walls protrude seaward from the cliff to the left (east) and right (west) of the ashlar wall (Fig. 6). This complex of three walls was perhaps part of a 'staircase' building, as a few remaining horizontal stone slabs appear as steps between these wall remains.

The position of field section 1 is indicated on Fig. 6 to the right (west) of the 'staircase' building. A geoarchaeological deposit is visible here above the hard conglomerate in between two wall remnants, which are about 3 m apart at their base on top of the conglomerate, about 1 m above current sea level. The section has a thickness of 2.20 m in between the base conglomerate and the vegetation cover on top.

Undisturbed micromorphology samples were taken in 2001 from the upper part of section 1. The samples were collected in

rather fine sediment, mixed with coarser components, at the following stratigraphic position: 10 cm above the uppermost stone of the wall remnant west of the ashlar wall, 10 cm below a horizontal stone slab – possibly a step of the staircase, about 40 cm below the vegetation cover. The position of this sample is *ca.* 1.70 m above the base conglomerate and 2.60 m above current sea level. The samples were impregnated by epoxy in a specialized lab to enable the making of thin sections. Microscopic studies of these thin sections from the upper part of section 1 revealed marine micro-fauna, including coralline algae (Fig. 15e), foraminifera (Fig. 15f) and inter-tidal zone components, such as pieces of cemented beach-rock and rounded beach sand in these multi-modal deposits.

The arrow at section 1 (Fig. 6) indicates the position where three imbricated cattle bones were found, shown in detail in Fig. 7, at a stratigraphic level of 60 cm above the base conglomerate and 1.50 m above sea level. Two cattle bones were sampled and dated by radiocarbon at the University of Groningen. The average non-calibrated ^{14}C date of 3350 ± 25 BP (Table 4, see Section 7.3) is strikingly similar to the average ^{14}C date of the Santorini eruption in radiocarbon years: 3350 ± 10 BP (Bronk Ramsey et al., 2004).

Fig. 7 of field section 1 shows a rather chaotic mixture of fine particles and coarse components – up to *ca.* 15 cm – of an astonishingly variegated nature, including building debris, stone slabs, ceramic sherds, wall plaster, small stones, rounded pebbles, and the three cattle bones. An outstanding feature is the widespread *imbrication* of the various course components. The term (contact) imbrication is used in sedimentology when pebbles or boulders overlap each other in a way similar to roof tiles or shingles (Johansson, 1976). Imbrication is caused by strong water currents. Therefore, it is an important diagnostic characteristic in palaeo-sedimentary studies. The imbrication of large particles like pebbles in a stream deposit may indicate the ancient flow direction (Johansson, 1976; Todd, 1996). Even the cattle bones in field section 1 occur in an imbricated position, overlain by overlapping ceramic sherds (Fig. 7). Imbrication of ceramic sherds and other archaeological objects has not been reported previously as far as we know. Deposition of pottery sherds below sea level on the shallow shelf by a tsunami that struck Caesarea, the harbour of Herod the Great, has been reported (Reinhardt et al., 2006).

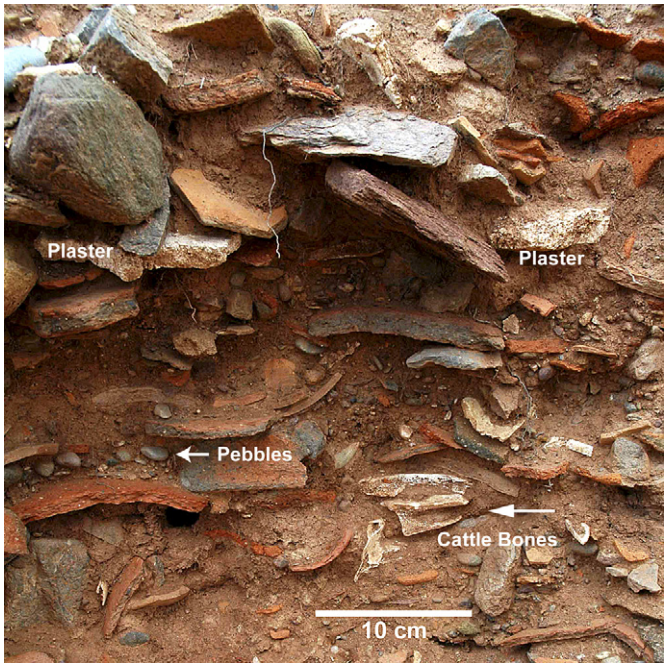

Fig. 7. The lower part of field section 1 at the Promontory, showing multi-modal chaotic deposits with imbrication – indicative of strong water flows during deposition – of stone slabs, wall plaster, ceramic sherds and three cattle bones, dated by ^{14}C to the time range of the Minoan Santorini eruption.

Another significant feature indicating movement by water in field section 1 is a discontinuous layer of rounded pebbles and smaller rounded stones, visible in between imbricated ceramic sherds to the left of the cattle bones (Fig. 7).

All these above mentioned features are *not* indicative of normal cultural formation processes in archaeology (Schiffer, 1987). Both imbrication and the chaotic multi-modal make-up of the geoarchaeological deposits in field section 1 at the Promontory do match tsunami signatures (Dominey-Howes, 2004; Scheffers and Kelletat, 2004; Dominey-Howes et al., 2006). The microscopic findings of coralline algae, foraminifera, cemented beach-rock and rounded beach sand in the upper part of field section 1 also fit tsunami signatures.

Sea storm deposits cannot account for imbrication of large objects and non-sorting of particles. Storm inundation is a gradual process, involving many waves, which transport sediment primarily as bed load by traction, leaving numerous discrete layers but not a single rather homogeneous deposit (Morton et al., 2007), containing both large objects and clay particles, as in field section 1 at the Promontory. The isolated geomorphological position of the Promontory and East Beach hillocks does not allow deposition by river or runoff flooding. In conclusion, it seems that tsunami inundation alone can account for our findings. Moreover, the imbricated cattle bones in these tsunamigenic deposits have the same radiocarbon age as the LM IA Santorini eruption.

4.3. Promontory: field section 2

Fig. 6 shows the location of field section 2 at the Promontory, situated left (east) of the 'staircase' building. The arrow of section 2 indicates the approximate level where volcanic ash was found, at a stratigraphic position ranging from *ca.* 30 to 80 cm above the hard conglomerate, about 1.75 m above current sea level (Fig. 6). Our detailed geochemical investigations proved that the volcanic ash at this level originated from the LM IA Santorini eruption (see Section 6).

The volcanic ash appears as intraclasts of soft fine-grained sediment with a light grey color (Munsell 5Y 7/1). The intraclasts range in size from a few millimeters up to about 10 cm and may have a rather sharp boundary or are diffusely mixed with the surrounding fine sediment that has a reddish-brown color (Figs. 8, 9). The volcanic ash intraclasts were only found in the lower part of the *ca.* 2 m thick geoarchaeological layer at section 2, composed of a mixture of fine particles and coarse components such as stones and ceramic sherds. Isolated shells

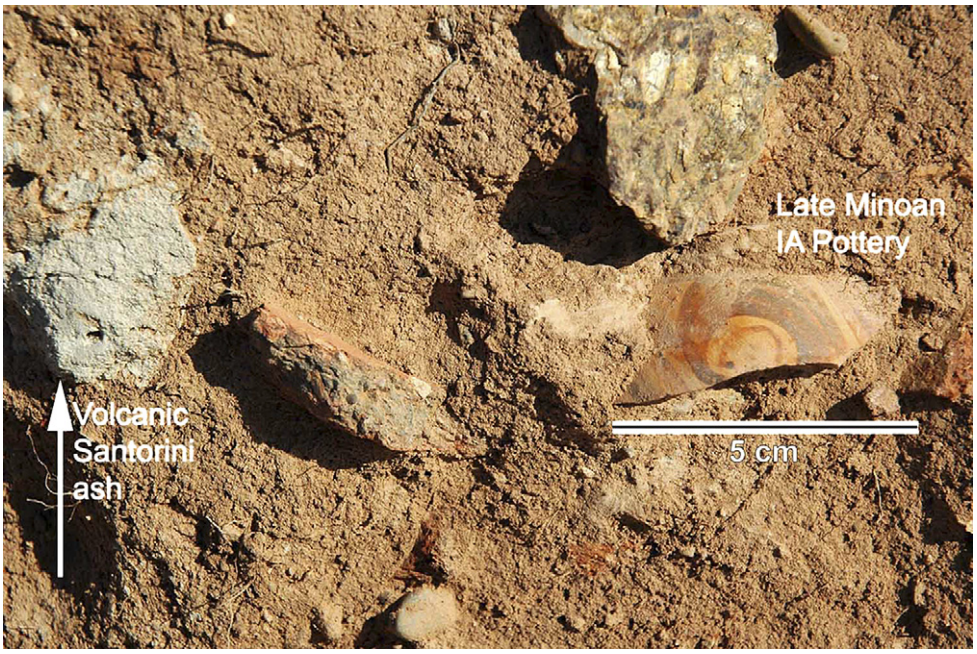

Fig. 8. The lower part of field section 2 at the Promontory, showing multi-modal deposits with intraclasts of volcanic Santorini ash and a diagnostic LM IA ceramic sherd.

were noticed occasionally (Fig. 9), as well as pieces of bone, but usually in a thin layer of scree near the base of the section and, therefore, not *in situ*.

Undisturbed samples were taken by Bruins in 2001 of volcanic ash intraclasts and the surrounding fine sediment – all *in situ*. The samples were impregnated by epoxy in a specialized lab and subsequently thin sections were prepared. Micromorphological and petrological investigations of the thin sections showed that the volcanic ash in the intraclasts consists of rather pure and fresh appearing volcanic glass with some minerals (Fig. 15d). The volcanic ash is found also randomly mixed in the surrounding reddish-brown sediment. Sharp contacts between volcanic ash intraclasts and reddish-brown sediment are visible in Fig. 15a.

The small size of the individual volcanic ash particles, ranging from fine silt up to sand fits initial airborne transport from the LM IA Santorini eruption, as studied by Wilson (1972) and Bond and Sparks (1976). The largest volcanic particle we found is a sand-size piece of pumice, 1.5 × 0.8 mm, visible in Fig. 15a to the right and enlarged in Fig. 15b. Bond and Sparks (1976) made a theoretical assessment of the maximum size of airborne tephra that could have reached Crete and they came to the following conclusion: "Even if the wind speed had been 50 m/s (jet stream velocities) to the south-east, calculations (Wilson, 1972) indicate that the maximum particle size to reach Crete could only have been around 2 mm" (Bond and Sparks, 1976, p. 15). Our "ground-truth" microscopic studies of volcanic ash found at Palaikastro in eastern Crete agree very well with this theoretical evaluation.

The volcanic ash intraclasts appear in a chaotic multi-modal sedimentary context together with fine sediment, as well as large objects such as stones and ceramic sherds. Fig. 8 shows a diagnostic LM IA ceramic sherd with a dark-on-light foliate scroll, situated near a volcanic ash intraclast. Similar pottery has also been found with redeposited Santorini ash in the excavated part of Minoan Palaikastro (MacGillivray et al., 1992, p. 136, Fig. 15). Fig. 9 shows a marine shell (*Patellidae*) near another volcanic ash intraclast. This shell was dated by ^{14}C (Table 4), as already mentioned above in the synopsis, and

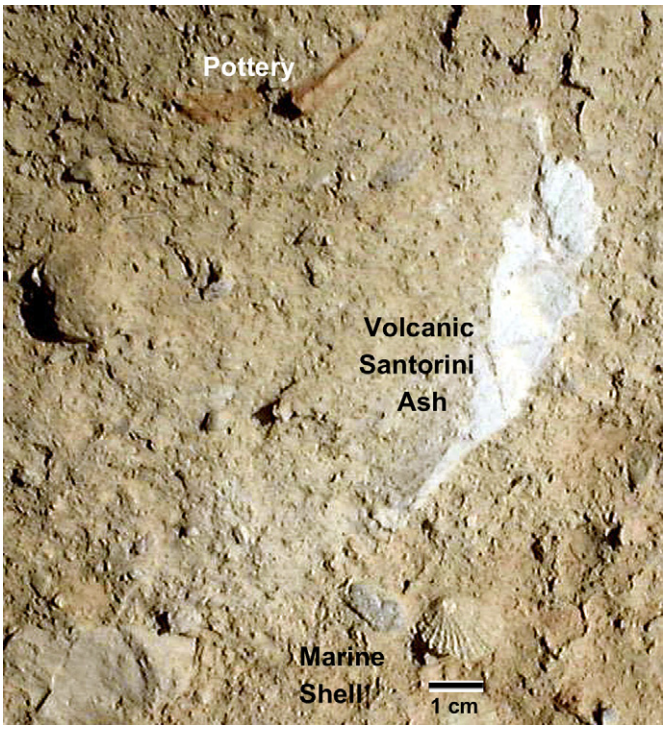

Fig. 9. The lower part of field section 2 at the Promontory, showing multi-modal deposits with intraclasts of volcanic Santorini ash and a marine *Patellidae* shell, dated by ^{14}C to the time range of the Minoan Santorini eruption.

yielded a result similar to the radiocarbon date of the LM IA Santorini eruption (see Section 7.3).

The non-sorted multi-modal make-up of field section 2, like field section 1 at the other side of the 'staircase' building, fits a tsunami signature (Scheffers and Kelletat, 2004). Moreover, the presence of intraclasts – composed of volcanic ash – in the lower parts of the geoarchaeological layer matches another tsunami signature (Dominey-Howes, 2004; Dominey-Howes et al., 2006). The sea surrounds the Promontory and one may ask whether storms could be responsible for these deposits? A study by Morton et al. (2007), aimed to distinguish tsunami and storm deposits from each other, concluded that mud intraclasts are strong evidence of tsunami deposition. The mud in our case is fine-grained volcanic ash, which must have been present to enable the formation of intraclasts by the tsunami, but the principle appears the same. Sediment transport during sea storms is primarily as bed load by traction (Morton et al., 2007), which does not lead to non-sorted chaotic deposits with intraclasts.

Moreover, time wise, the *in situ* marine shell (*Patellidae*), dated by radiocarbon, the adjacent volcanic ash intraclast (Fig. 9), the diagnostic ceramic sherd next to another volcanic ash intraclast (Fig. 8), all fit the time of the LM IA Santorini eruption. Also the dated cattle bones of section 1 had a radiocarbon age similar to the latter eruption. This multiple evidence supports a tsunami event during the LM IA Santorini eruption that struck the Palaikastro area.

4.4. East Beach: field section 3

The hillock that exists on the Promontory continues southward along the East Beach (Fig. 5), rising to levels of *ca*. 9 m above sea level at the highest points, marked by hard conglomerates and cemented cross-bedded aeolianite sandstone. The East Beach cliff is usually higher and more vertical than the cliff along the Promontory, but becomes progressively lower southward (Fig. 5). Further on the cliff disappears and only a few isolated remnants remain along the East Beach. Continuing south-eastward another hillock with cliff, isolated from the hinterland, exists along the coast (Fig. 5). The ancient town covered the coastal area from the tip of the Promontory south-eastward along the East Beach over a length of about 300 m in the Late Minoan period (MacGillivray et al., 1984, p. 140).

A geoarchaeological layer of mixed composition forms the upper layer on the East Beach cliff at many sections, but not everywhere. The layer is usually without visible internal stratification and without sorting and includes fine reddish-brown sediment, settlement debris, large and small (building) stones, ceramic sherds, cups, wall plaster, flooring pieces, rounded (beach) pebbles, and sometimes a marine shell. This geoarchaeological layer occurs at elevations ranging from beach level to a maximum height of *ca*. 7 m, but is absent at the highest parts of the cliff and various other segments. Its thickness ranges from less than 0.5 m to more than 2 m.

Field section 3 along the East Beach is located in the comparatively lower southern part of the cliff (Figs. 3, 5, 10). The boundary between the mixed geoarchaeological layer and older geological strata is indicated by a white line (Fig. 10). A large concentration of rounded pebbles, *ca*. 3.5 m above sea level, is visible above wall remains of a Minoan building (Fig. 10). This is not an ordinary stream channel deposit. The land surface behind the East Beach cliff slopes down to a valley that separates the Promontory and East Beach hillocks from the hinterland (Fig. 5). Therefore, this channel with rounded pebbles could not have originated

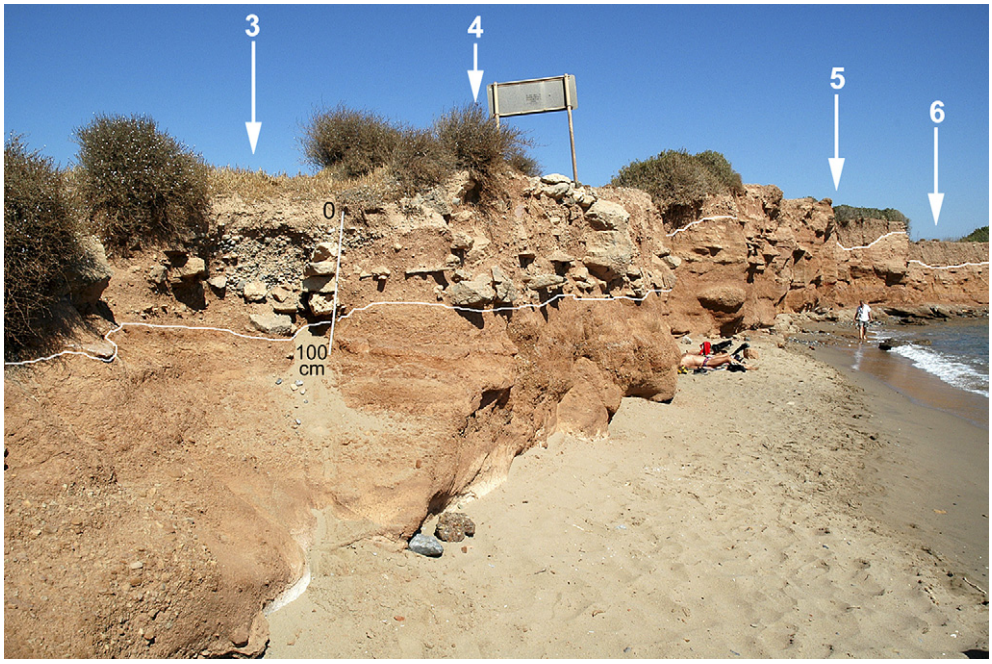

Fig. 10. The East Beach cliff with field sections 3–6.

in the Mount Petsofas catchment area, fed by rainfall and surface runoff.

The only alternative is that the deposit was created by seawater inundation. Indeed the pebbles are too well rounded for fluviatile stream channels, even if the channel had extended a few hundred meters to Mount Petsofas. The degree of roundness of the pebbles is indeed similar to those lying on the beach in the area, based on our observations. Moreover, the pebble deposit is *not* well sorted, because the deposit displays many different particle sizes, including large stones of about 8 cm, rounded pebbles in the range of 2–4 cm, as well as many smaller stones and gravel, besides fine reddish-brown material of silt-clay size (Fig. 11).

A striking feature of the deposit is the overlapping position – imbrication – of a number of pebbles, indicative of strong water flow (Johansson, 1976; Todd, 1996). This is clearly visible in the top left and bottom right parts of Fig. 11. Recent deposits from a tsunami that hit northern Japan in 1993 show landward imbrication of pebbles, as well as seaward imbrication, caused by run-up and backflow of the seawater, respectively (Nanayama et al., 1998, 2000).

This mixed pebble deposit overlies Minoan building and wall remains (Fig. 10) at *ca*. 3.50 m above current sea level. Both archaeological surveys in the area (MacGillivray et al., 1984) and other studies (Sneh and Klein, 1984; Flemming and Webb, 1986; Kayan, 1988, 1991) indicate that sea level in Late Minoan times was about 1–2 m lower than today. Hence seawater flow depths must have been at least 5 m and possibly more to drop this mixed pebble deposit that high on land over the remnants of a Minoan building. Flow depths during severe sea storm inundation are commonly below 3 m from a global perspective (Morton et al., 2007). The east coast of Crete is relatively sheltered from dominantly western storms and sea storm inundation here is probably less likely.

Fig. 11. The upper part of field section 3 at the East Beach cliff, showing rounded (beach) pebbles in a multi-modal deposit overlying wall remains of a Minoan building, *ca*. 3.5 m above current sea level. Some pebbles show imbrication, indicative of strong water currents during deposition.

Moreover, sediment transport during sea storms, usually by traction, causes rather well-sorted deposits (Morton et al., 2007). Therefore, it seems that only a tsunami can account for the mixed pebble deposit overlying the remains of a Minoan building along East Beach field section 3.

4.5. East Beach: field section 4

Looking at Fig. 10, it can be seen that the mixed layer with the pebble deposit continues towards field section 4, showing a chaotic mixture of wall remnants and large dislocated building stones, as well as other pebbles. Fig. 12 gives a close-up of section 4. The white line indicates the boundary between the mixed geoarchaeological layer and the underlying geological strata. The latter layers look well sorted (Fig. 12). The stratum immediately below the geoarchaeological layer is fine-grained without gravel. The next underlying stratum shows gravel, but only within a restricted size range of a few centimeters.

It is clearly visible that the geoarchaeological layer on top has a completely different make-up, being multi-modal and chaotic in terms of sorting (Fig. 12). This characteristic fits a tsunami signature (Scheffers and Kelletat, 2004). Nevertheless, one might argue that the make-up of the upper layer in field section 4 is simply due to archaeological formation processes, as compiled for example by Schiffer (1987). If that would be the case, one would expect various types of stratification with clear boundaries, such as living floors. Yet the upper layer, though chaotic and multi-modal, does not show discernable internal layering. The only distinct boundary is the erosional contact – basal unconformity – with the underlying sediment, as indicated by the irregular position of the white line (Fig. 12). This erosional contact fits another tsunami signature (Dominey-Howes, 2004; Dominey-Howes et al., 2006). Moreover, the large stones in the lower part of the geoarchaeological layer may be considered as a third tsunami signature, *i.e*. reworked material (Dominey-Howes, 2004; Dominey-Howes et al., 2006), apparently from destroyed walls.

4.6. East Beach: field sections 5 and 6

Further northward along the East Beach cliff are field sections 5 and 6 (Figs. 3, 5, 10). The non-sorted geoarchaeological layer on top of the hillock stretches here continuously over a considerable distance. The erosional basal contact with the underlying geological strata is indicated by the white line (Fig. 13). The geoarchaeological layer contains again a chaotic mixture of fine reddish-brown sediment, ceramic sherds, cups, stones, pebbles and sometimes marine shells. The cliff at this position along the East Beach is higher than the previous section and the surface of the geological layer is about 7 m above current sea level, *i.e*. 8–9 m above Late Minoan sea level (Sneh and Klein, 1984; Flemming and Webb, 1986; Kayan, 1988, 1991). A marine shell with eroded angular edges (probably *Patellidae*) was found by Bruins in 2006 on top of field section 5 (position indicated by the white arrow with letter S in Fig. 13), about 6.50 m above current sea

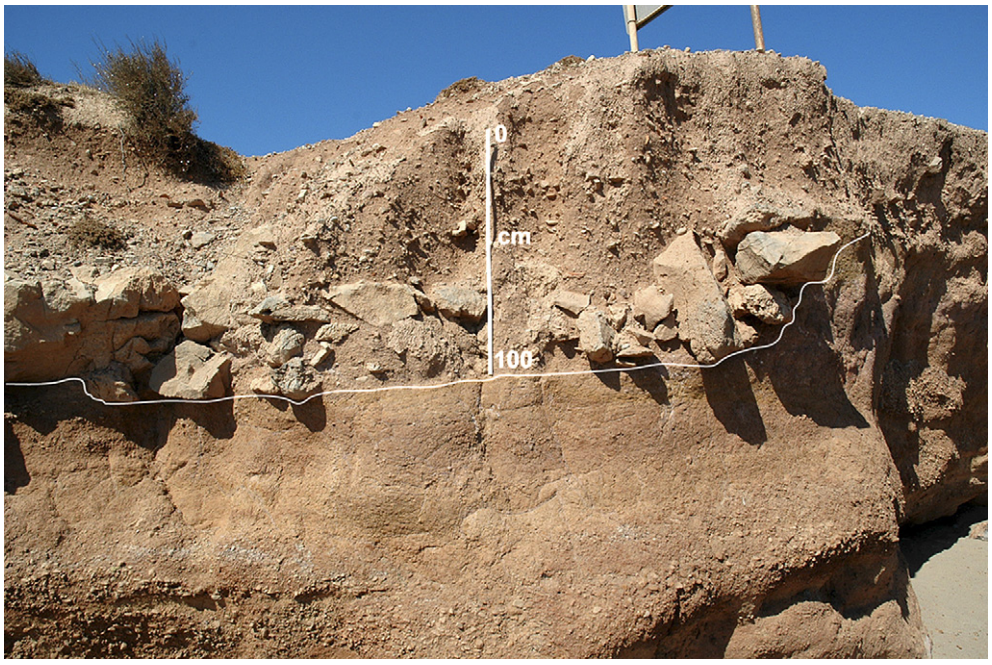

Fig. 12. Field section 4 at the East Beach cliff. The white line indicates the erosional contact – basal unconformity – between the multi-modal chaotic geoarchaeological layer and the underlying geological strata. Wall remains and dislocated building stones are present as reworked material in the lower part of the geoarchaeological layer.

level. This shell (Fig. 14) has so far not been dated and might be out of context, but other marine shells have been noted in the layer. Angular shell fragments are typical in a historical tsunami deposit on the marine shelf at Ceasarea, Israel (Reinhardt et al., 2006).

Wall remnants are not evident in field sections 5 and 6, but three flat stones are visible at the erosional basal contact of the geoarchaeological layer with the underlying stratum (Fig. 13, see black arrows). Two of these stones touch each other and the third lies a bit further in the same position and at the same level. Perhaps these were flagstones, signifying an ancient archaeological surface that existed here before accumulation of the mixed geoarchaeological layer.

In conclusion, the latter layer in field sections 5 and 6 is too high for storm deposits, but contains three possible tsunami signatures: basal unconformity, individual marine shells (Dominey-Howes, 2004; Dominey-Howes et al., 2006) and multi-modal chaotic composition (Scheffers and Kelletat, 2004). Such a sedimentary make-up is incompatible with sea storm deposits (Morton et al., 2007).

5. Volcanic Santorini ash deposits in the excavated inland part of Minoan Palaikastro

Volcanic ash was discovered during previous years in the course of archaeological excavations (MacGillivray et al.,

Fig. 13. Field sections 5 and 6 along the East Beach cliff. The white line indicates the erosional contact – basal unconformity – between the multi-modal chaotic geoarchaeological layer and the underlying geological strata. Three flagstones (black arrows) are present at the erosional contact. A *Patellidae* shell was found on the surface of section 5 (white arrow with letter S), 6.50 m above current sea level.

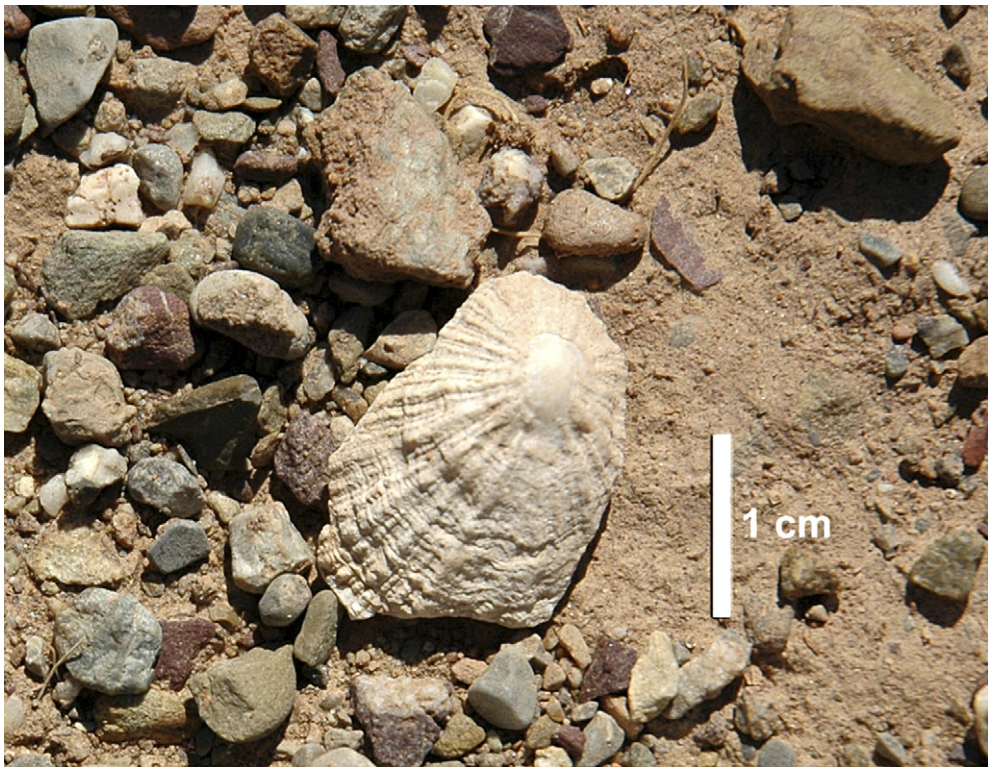

Fig. 14. Close-up of the surface of field section 5 along the East Beach cliff, showing the *Patellidae* shell with angular eroded edges.

1991, 1998) at the main excavation site, situated 9–12 m above sea level, about 300 m inland from the Promontory peninsula and East Beach coast (Figs. 3, 4). Distinct but discontinuous layers of light grey volcanic ash (Munsell color 5Y 7/1) were found in the Main Street, in open areas in Building 6 (MacGillivray et al., 1998), and outside Building 7 (MacGillivray et al., 1991). The approximate locations of these excavated buildings are indicated in Fig. 3.

The volcanic ash appears sometimes mixed with reddish-brown sediment in irregular patterns, reminiscent of the volcanic ash intraclast found in reddish-brown sediment near the basis of field section 2 at the Promontory. The thickness of discrete and rather pure volcanic ash layers is up to 12 cm. Our geochemical investigations, conducted by Keller and Klügel, proved without any doubt that the volcanic ash in the above locations at the archaeological excavation site originated from the LM IA Santorini eruption, as presented in detail in Section 6.

Undisturbed samples were taken from layers containing volcanic ash for microscopic studies. These samples were impregnated by epoxy in specialized labs to enable the making of thin sections with a large size of 8 × 8 or 6 × 8 cm. The volcanic ash dominantly consists of tiny volcanic glass particles of irregular and elongated shape, besides fine pumice shards, mineral and rock components. A micro-photograph of volcanic ash from trench EM-85 in Building 6 is shown in Fig. 15d.

Another micromorphology sample, taken from a volcanic ash layer at the north face of Building 7, is shown in Fig. 15c. The microscopic magnification of the latter figure is much less than the former, showing the layered micro-stratigraphy of the volcanic ash deposit, rather than the individual particles. The size of the fine volcanic particles, usually silt size and sometimes sand-size below 2 mm, fits original airborne deposition (Wilson, 1972; Bond and Sparks, 1976). The question is whether the layered micro-stratigraphy (Fig. 15c) represents original airborne sedimentation during the LM IA volcanic eruption or subsequent redeposition in water?

Detailed archaeological studies of the architectural and related archaeological phases of Buildings 6 and 7 are still continuing. Future publications will probably be able to show the location and stratigraphy of the volcanic ash vis-à-vis the original micro-topography of the nearby ancient streets and buildings in minute detail.

It can be stated here that the volcanic ash layers mark a mature stage of the LM IA period in a number of excavated locations at Palaikastro, as noted during previous excavations (MacGillivray et al., 1998). The layering or mixed appearance of the volcanic ash with reddish-brown sediment, as well as its stratigraphic relationships with overlying and underlying strata, seem to indicate redeposition in open spaces by water. Possible tsunami action was already suggested by MacGillivray et al. (1987, pp. 150–151), based on the excavations of Building 2, as pointed out also by Driessen and Macdonald (1997). Sea storms, usually coming from westerly directions, are unlikely to have swept here at the eastern coast of Crete to elevations of 9–12 m above current sea level, 300 m inland from the shore.

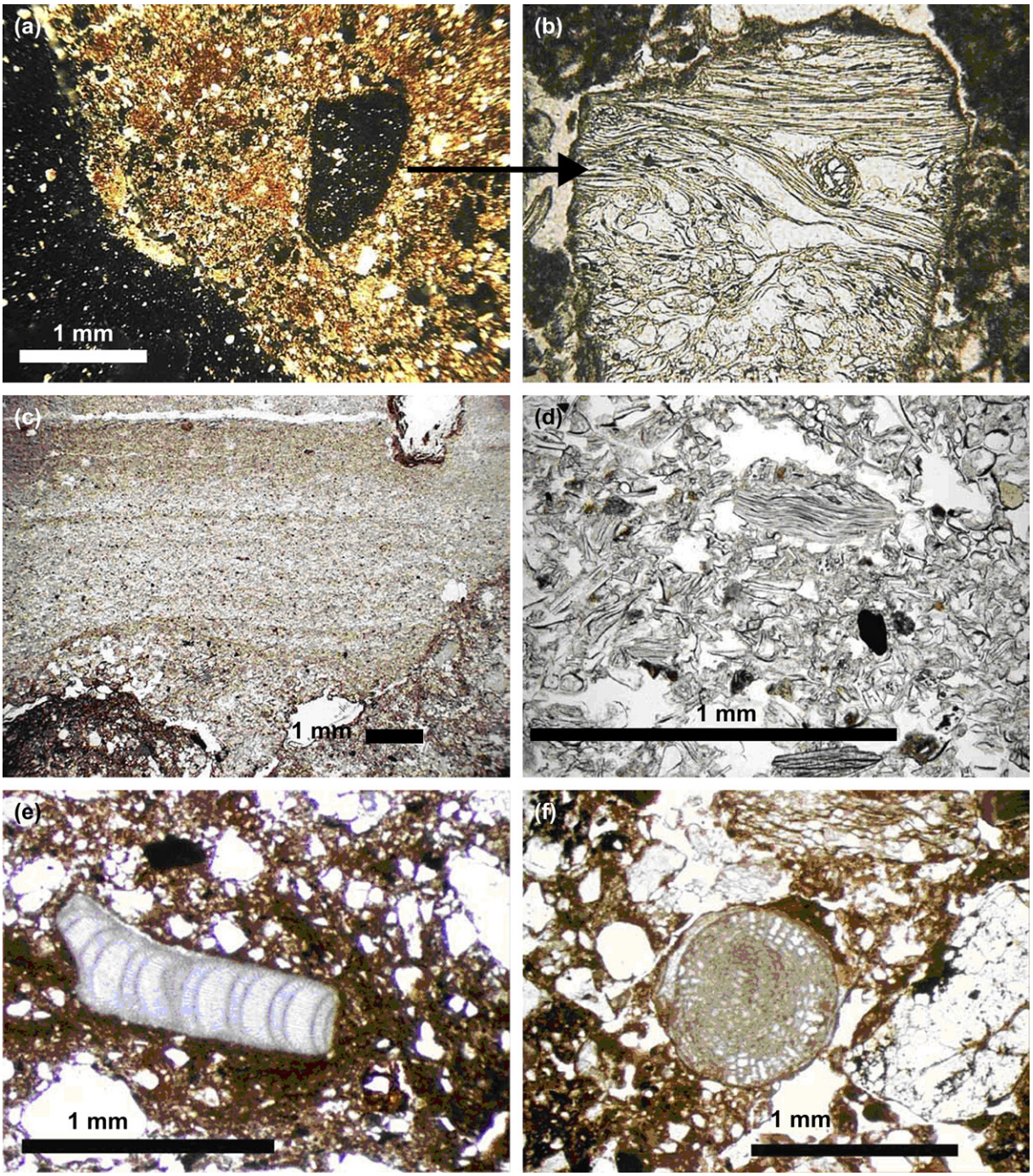

Fig. 15. Micro-photographs from thin sections. (a) Field section 2 at the Promontory, showing reddish-brown sediment and part of an intraclast of volcanic Minoan Santorini ash (black) in crossed polarized light; a single pumice particle (black) appears right of centre. (b) Close-up of the same pumice particle in plain polarized light (ppl); length of the photograph is 1 mm. (c) Building 7, north face, in the archaeological excavation area, showing layered micro-stratigraphy in volcanic Santorini ash (ppl). (d) Building 6, trench EM-85, in the archaeological excavation area, showing volcanic Santorini ash composed of irregular shaped volcanic glass shards, fibrous and vesicular pumice particles, as well as volcanic minerals (ppl). (e) Field section 1 at the Promontory, upper part of the 'staircase' building remains, showing branching coralline algae of marine origin situated in a matrix of fine reddish-brown sediment (ppl). (f) Same location in the 'staircase' building, showing an originally round marine *Planorbulinella* foraminiferam in a matrix of fine reddish-brown sediment (ppl).

6. Geochemistry of the volcanic ash

The geochemical composition of the redeposited volcanic ash, found at the Promontory and in excavated parts of Minoan Palaikastro, was investigated in order to verify the source, as each volcanic eruption has its own unique geochemical signature. The chemical fingerprinting was carried out by single shard discrete point analysis by Electron Probe Micro-Analysis (EPMA) for major elements at the University of Freiburg, and by Laser Ablation Inductively Coupled Plasma Mass

Spectrometry (LA-ICP-MS) for trace elements at the University of Bremen.

Microprobe analyses were conducted with a CAMECA SX100 wavelength dispersive electron probe. Preparation of polished thin sections for analysis was done directly from the epoxy impregnated blocks. To avoid loss of alkalis, a beam diameter of 10 μm and a beam current of 10 nA was consistently applied. Calibration was undertaken against international oxide, mineral and glass standards (Jarosewich et al., 1980). Summary major element EPMA data of four different tephra samples from Palaikastro are reported in Table 2 and compared with Minoan tephra from Santorini and other locations with distal ash layers (Keller, 1980b; Druitt et al., 1999; Eastwood et al., 1999), all measured by microprobe point analyses of single glass shards. There is excellent agreement between all data (Table 2), proving unequivocally that the volcanic ash found at the Promontory and excavated parts of Palaikastro are all derived from the Minoan Santorini eruption.

LA-ICP-MS analyses of single glass shards (Eastwood et al., 1998; Pearce et al., 2002) were carried out using a 266 nm UV laser connected to an Element2. Ablation conditions included a pulse rate of 5 Hz, a crater diameter of *ca.* 40 μm, and He as carrier gas in the ablation cell (0.39 l/min) with subsequent addition of Ar (1 l/min). Rhyolitic glass ATHO-G was used for external calibration with Ca as internal standard element, and dacitic glass StHs6/80G was regularly analyzed as a monitor, using the values by Jochum et al. (2000). Four different tephra samples were analysed from Palaikastro and one sample from southern Thera of the fourth (ignimbrite) eruption phase (Table 3). The concentrations of all analyzed trace elements from Palaikastro glass shards perfectly agree with each other within one standard deviation and also with the Thera (Santorini) glass shards. There is also excellent agreement between ratios of incompatible trace elements, which are more reliable chemical fingerprints than absolute concentrations (Pearce et al., 2002).

7. Dating the geoarchaeological tsunami deposits

The reasons for the divergence between radiocarbon dating and archaeo-historical dating during the mid-second millennium BCE in the Eastern Mediterranean and Near East have not yet been resolved (Warren and Hankey, 1989; Bruins and Mook, 1989; Manning, 1999; Van der Plicht and Bruins, 2001; Bietak, 2003; Bietak and Höflmayer, 2007; Wiener, 2003, 2007; Bruins and Van der Plicht, 2003; Bruins, 2007; Bronk Ramsey et al., 2004; Manning et al., 2006; Friedrich et al., 2006). This problem complicates matters, because mixing dates from the two principal chronological systems – Egyptian Calendar and radiocarbon dating – may lead to erroneous correlations and conclusions. The most precise and accurate calibrated ^{14}C date so far for the Santorini eruption is 1627–1600 BCE, based on radiocarbon analysis and wiggle matching of tree rings in an olive tree found covered by tephra on Santorini (Friedrich et al., 2006).

7.1. Geological dating criteria

A geological criterion for dating the geoarchaeological deposits, characterized by tsunami signatures, is the presence of reworked Minoan Santorini ash. The fall-out of volcanic ash over eastern Crete during the Santorini eruption was estimated to have been about 5 cm thick, according to geographic extrapolation of volcanic ash data, mainly from deep-sea sediments (Watkins et al., 1978; Thorarinsson, 1978; McCoy, 1980). Such a thin layer will not easily remain preserved in the open landscape, as volcanic ash is susceptible to wind and water erosion, particularly in arid and semi-arid hilly regions (Inbar et al., 1995). The Palaikastro area in eastern Crete is famous among surfers for its strong winds.

Volcanic ash particles originating from the Minoan Santorini eruption have been found dispersed in Cretan soils (Vitaliano and Vitaliano, 1974; Betancourt et al., 1990). But

Table 2
Major element analyses by electron microprobe (University of Freiburg) of single glass shards, correlated with the Minoan eruption of Thera (Santorini)

	Palaikastro Promontory, BC5/1 ($n=24$)	Palaikastro Promontory, BC1-9a ($n=19$)	Palaikastro Building, 7 North ($n=15$)	Palaikastro Trench, EM-85 ($n=14$)	Palaikastro, ∅ ($n=72$)	SD	Thera[b] (Plinian phase, $n=4$)	Thera[a] (Plinian phase, $n=7$)	Kos[b] ($n=3$)	Gölhisar[c] (n = 67)
SiO_2	73.32	73.20	73.25	73.21	73.25	0.34	73.00	73.44	73.36	73.61
TiO_2	0.29	0.29	0.30	0.29	0.29	0.04	0.32	0.31	0.33	0.29
Al_2O_3	14.13	14.06	14.02	14.14	14.09	0.17	14.13	14.46	14.19	14.02
FeOt	2.08	2.11	2.11	2.15	2.11	0.11	2.13	2.05	2.08	2.04
MnO	0.07	0.07	0.08	0.08	0.07	0.03				0.07
MgO	0.30	0.31	0.30	0.32	0.31	0.03	0.34	0.25	0.32	0.28
CaO	1.42	1.43	1.44	1.45	1.43	0.08	1.48	1.56	1.41	1.40
Na_2O	4.78	4.91	4.90	4.76	4.83	0.23	4.79	4.81	4.55	4.76
K_2O	3.29	3.30	3.29	3.29	3.29	0.11	3.45	3.16	3.40	3.24
Cl	0.31	0.31	0.31	0.30	0.31	0.03	0.37		0.37	0.30
Sum	100.00	100.00	100.00	100.00	100.00		100.00	100.00	100.00	100.00

All analyses by electron microprobe, results in weight percentages normalised to 100%, volatile-free. FeOt, total Fe calculated as Fe^{2+}; *n*, number of point analyses; SD, standard deviation; blank, not analysed or not detected.

[a] Druitt et al. (1999).

[b] Keller (1980b).

[c] Eastwood et al. (1999).

Table 3
Trace element analyses by Laser Ablation Inductively Coupled Plasma Mass Spectrometry (University of Bremen) of single glass shards and minute pumice shards, correlated with the Minoan eruption of Thera (Santorini)

	Palaikastro Promontory, BC5/1 ($n=17$)	Palaikastro Promontory, BC1-9a ($n=8$)	Palaikastro Building 7, North ($n=12$)	Palaikastro Trench, EM-85 ($n=21$)	Palaikastro ∅ ($n=58$)	Palaikastro standard deviation, SD	Thera (Minoan Ignimbrite phase)	Turkey[a] (distal tephra)
Rb	113	109	115	106	110	10.8	108	116
Sr	65.4	66.3	65.9	67.2	66.3	4.70	63.8	56.9
Y	45.7	39.0	44.0	47.7	45.2	4.92	41.4	36.3
Zr	354	314	346	381	357	36.0	340	287
Nb	11.7	11.6	11.2	11.2	11.4	0.92	12.0	10.1
Ba	547	547	509	548	539	47.6	568	461
La	30.7	28.7	29.2	31.8	30.5	2.82	29.9	32.1
Ce	59.8	58.5	55.9	58.8	58.4	5.82	60.9	50.5
Pr	6.47	6.16	6.17	6.52	6.39	0.57	6.51	6.02
Nd	25.7	23.8	24.5	26.5	25.5	2.47	25.2	24.6
Sm	5.76	5.36	5.78	6.15	5.85	0.61	5.80	5.39
Eu	1.00	0.89	0.93	0.90	0.94	0.11	0.96	0.80
Gd	6.11	5.43	5.97	6.51	6.13	0.78	5.88	5.35
Tb	1.06	0.90	0.95	1.07	1.02	0.12	0.98	1.01
Dy	6.80	5.68	6.37	6.86	6.58	0.78	6.32	6.61
Ho	1.51	1.30	1.47	1.56	1.49	0.20	1.45	1.56
Er	4.94	4.31	4.60	5.21	4.88	0.69	4.60	4.52
Tm	0.81	0.70	0.74	0.81	0.78	0.13	0.74	0.74
Yb	5.39	4.71	5.29	5.75	5.41	0.76	5.06	5.29
Lu	0.93	0.72	0.84	0.91	0.87	0.14	0.81	0.92
Hf	9.25	8.09	8.56	9.99	9.21	1.21	8.48	7.05
Ta	0.92	0.93	0.94	1.02	0.97	0.16	0.99	1.01
Pb	20.2	20.0	29.0	20.1	21.7	5.88	18.3	
Th	20.4	19.0	20.0	23.1	21.1	2.88	20.2	16.6
U	6.19	5.86	5.85	5.89	5.97	0.88	6.19	5.52
Ba/Nb	47.0	47.4	45.2	48.9	47.4	2.80	47.6	45.7
Zr/Nb	30.5	27.3	30.5	34.0	31.3	3.32	28.6	28.5
Zr/Th	17.4	16.5	17.2	16.6	16.9	0.94	16.9	17.3
Zr/Y	7.77	8.06	7.84	7.99	7.9	0.28	8.22	7.92
Hf/Ta	10.07	8.76	9.03	9.96	9.6	1.20	8.59	6.98
La/Ce	0.51	0.49	0.52	0.54	0.5	0.04	0.49	0.64
La/Lu	33.2	39.9	34.7	35.5	35.3	3.40	36.9	35.0
La/Nb	2.64	2.49	2.57	2.84	2.7	0.23	2.51	3.18
Ce/Yb	11.2	12.5	10.8	10.3	11.0	1.15	12.1	9.54
Th/Nb	1.76	1.65	1.77	2.06	1.9	0.22	1.69	1.64
Th/U	3.32	3.25	3.42	4.00	3.6	0.50	3.28	3.00
Nb/Y	0.26	0.30	0.26	0.24	0.3	0.03	0.29	0.28
Nb/U	1.89	1.97	1.94	1.95	1.9	0.16	1.94	1.83

All analyses by Laser Ablation ICP-MS; single element concentrations in μg/g; element ratios without dimension.
[a] Pearce et al. (2002).

distinct volcanic ash layers are *not* apparent in the open hilly landscape of Crete. It is clear that a tsunami cannot redeposit volcanic ash particles from a diluted presence in soils into discrete intraclasts and strata, as found at Palaikastro. Therefore, pure airborne volcanic ash must have been available as a layer across the landscape surface. Tsunami action seems to have occurred shortly after volcanic ash deposition in eastern Crete, possibly during the third or fourth eruption phase, when there is evidence for tsunami deposits on Thera (Druitt et al., 1999; McCoy and Heiken, 2000).

7.2. Archaeological dating criteria

The Santorini eruption occurred during the LM IA ceramic period (Doumas, 1983; Driessen and Macdonald, 1997, 2000). Archaeological excavations at the island of Mochlos along the north coast of eastern Crete revealed discrete volcanic ash layers in Late Minoan IA context (Soles and Davaras, 1990). At Palaikastro, a painted LM IA pottery sherd appeared *in situ* next to a clast of Santorini ash (Fig. 8) in field section 2 at the Promontory. This ceramic sherd with a dark-on-light foliate scroll is typical also of the pottery found with redeposited Santorini ash in excavated town layers (MacGillivray et al. 1992, p. 136, Fig. 15). Indeed LM IA pottery appears the youngest element found in such layers. Conclusive archaeological dating at the Promontory and East Beach hillocks would of course require systematic excavations, which have not been scheduled thus far. However, radiocarbon measurements of organic materials found exposed in the multi-modal geoarchaeological deposits gave convincing dating results (Table 4).

Table 4
Radiocarbon dates of cattle bones and marine shells from the Promontory at Palaikastro, dated by AMS at the University of Groningen (The Netherlands)

Field sample	Material	Species	Fraction dated	Lab no.	^{14}C Age (yr BP)	δ^{13}C	Note
PK-PR-1	Bone	Cattle	Collagen	GrA-30336	3310 ± 35	−20.81	
PK-PR-2	Bone	Cattle	Collagen	GrA-30339	3390 ± 35	−18.71	
BC-1-10	Shell	Patellidae	Carbonate	GrA-21607	3790 ± 60	2.48	
PK-prom-1-1	Shell	*Arca noae* Linneaus 1758	Carbonate	GrA-29592	105.5% ± 0.5	2.07	*
PK-prom-1-1	Shell	*Arca noae* Linneaus 1758	Carbonate	GrA-29598	107.0% ± 0.5	2.01	*, D
PK-prom-1-3	Shell	Patellidae	Carbonate	GrA-29593	4165 ± 40	3.59	
PK-prom-1-3	Shell	Patellidae	Carbonate	GrA-29599	4245 ± 40	3.93	D
PK-prom-2-11	Shell	*Monodonta turbinata*	Carbonate	GrA-29596	3625 ± 40	1.99	
PK-prom-2-11	Shell	*Monodonta turbinata*	Carbonate	GrA-29601	3540 ± 40	1.68	D
PK-prom-2-12	Shell	Muricidae	Carbonate	GrA-29602	3370 ± 40	0.06	
PK-prom-2-12	Shell	Muricidae	Carbonate	GrA-29597	3485 ± 40	0.03	D

*, modern value, reported in % instead of BP; D, duplicate measurement.

7.3. Radiocarbon dating of cattle bones from the Promontory

Radiocarbon dating was performed by AMS (Accelerator Mass Spectrometry) at the ^{14}C laboratory of the University of Groningen, the Netherlands (laboratory code GrA), in the framework of an ongoing regional ^{14}C dating project (Bruins and Mook, 1989; Van der Plicht and Bruins, 2001; Bruins and Van der Plicht, 2003; Bruins et al., 2003). The samples were pretreated using standard techniques. Collagen was extracted from the cattle bones and combusted to CO_2. Subsequently, the graphite targets for the ion source of the AMS (Aerts-Bijma et al., 2001) were prepared from the CO_2 gas. The AMS measures the $^{14}C/^{12}C$ and $^{13}C/^{12}C$ isotope ratios, enabling calculation of the radiocarbon ages (Van der Plicht et al., 2000), which are reported in BP, including correction for isotopic fractionation using the $\delta^{13}C$ values.

The imbricated *in situ* position of cattle bones and ceramic sherds in field section 1 at the Promontory (Figs. 6, 7) has already been described above. The average ^{14}C age of the two cattle bones (Table 4) is 3350 ± 25 BP. This result is in remarkable agreement with the average radiocarbon date in ^{14}C years of the Santorini eruption: 3350 ± 10 BP (Bronk Ramsey et al., 2004).

7.4. Radiocarbon dating of marine shells from the Promontory

Also marine shells were dated in Groningen by AMS, whereby the carbonate was extracted by an acid bath to obtain CO_2. Marine shells are less suitable for accurate dating in comparison to atmospheric (terrestrial) biological systems, because of the so-called reservoir effect. The radiocarbon age of a marine shell is approximately 400 years older than its real age. A value for the Mediterranean Sea surface radiocarbon reservoir age is 390 ± 80 yr (Siani et al., 2001). However, the reservoir effect can vary significantly, being younger in lagoons where continental freshwater enters the sea and older near places of upwelling of deep ocean water.

A Patellidae shell from field section 2 (Figs. 6, 8) was found embedded in the sedimentary matrix near an intraclast of volcanic Santorini ash and ceramic sherds. Its radiocarbon measurement (Table 4) gave a result of 3790 ± 60 yr BP (GrA-21607). Deducting the average marine carbon residence time of 400 years from the above result gives a date of 3390 ± 60 yr BP, which overlaps with the cattle bone dates (Table 4). Hence the actual age of this shell seems comparable to the ^{14}C age of the Minoan Santorini eruption.

Another Patellidae shell from a different erosive surface position near field sections 1 and 2 gave older dates of 4165 ± 40 yr BP (GrA-29593) and 4245 ± 40 yr BP (GrA-29599). A tsunami may of course scoop up and deposit shells older than the event. Other shells (Monodonta and Muricidae) found at the Promontory – *not in situ* – appear to be slightly younger than the Santorini eruption (Table 4), assuming a marine carbon residence time of 400 years. The Promontory is surrounded by the sea (Figs. 3–5) and storms or later tsunamis could have dropped these shells.

An *Arca noae* shell yielded a most interesting recent date, which can be related to the period of nuclear bomb tests in the atmosphere during the 1950s. This shell may have been dumped by a storm, a bird, a tourist or the most recent tsunami of 1956. Atomic bomb tests dramatically increased the radiocarbon content in the atmosphere and oceans until the test-ban treaty of 10 October 1963. Organic materials containing bomb peak amounts of ^{14}C can be dated rather accurately with radiocarbon. The shell – *Arca noae Linneaus 1758* – yielded a date of *ca*. 1955. A small tsunami hit Crete on July 9, 1956, caused by the combined action of a reactivated large normal fault to the south of Amorgos Island and earthquake induced slumping of sediment into an undersea trench (Galanopoulos, 1960; Ambraseys, 1960; Perissoratis and Papadopoulos, 1999; Dominey-Howes et al., 2000; Friedrich, 2000; Okal et al., 2004). Amorgos is situated north-east of Santorini (Fig. 1).

We questioned people living in the modern town of Palaikastro and some remembered this tsunami of 1956. Seawater flowed upward into the dry river valley near the town for more than 1 km inland. This bizarre phenomenon caused quite a stir, as witnesses away from the coast did not realize at first

the tsunami connection. Fish and other marine objects were deposited inland along the shore. Coastal vineyards and orchards were salted by seawater, rendering them useless for about 20 years. Otherwise, the comparatively small 1956 tsunami did not cause appreciable damage.

8. Modeling of the Minoan tsunami

Accurate modeling of tsunami inundation involves specification of an initial condition, detailed bathymetry and coastal topographic data. Given the uncertainty of the precise nature and size of tsunami triggers during the Minoan Santorini eruption, forward modeling by specifying initial conditions (Antonopoulos, 1992; Pareschi et al., 2006) is a mute proposition. Modeling ought to be based as much as possible on field evidence, as attempted before (McCoy et al., 2000).

Here, we present initial results of inverse modeling based on the newly discovered tsunamigenic deposits to infer the size of the initial wave. We used MOST (Titov and Synolakis, 1998; Synolakis and Bernard, 2006), a model extensively validated by laboratory and field data and with analytical solutions, to perform tsunami propagation and inundation calculations. MOST uses a system of three nested rectangular computational grids in geophysical coordinates, thus permitting efficient numerical solution over a wide area.

Regions far from the area of interest were modeled with coarser 1200 and 600 m outer grids, but for the specific study area near Palaikastro a finer 300 m resolution was used. Finer resolution was possible, as we conducted bathymetric surveys to augment our model. However, given the ill-posed nature of the inverse problem and the difficulties of regularizing it (Sigurdsson et al., 2006), we felt it would have been factitious to claim tens of meters in model accuracy, in a geophysical problem where uncertainties about the initial condition dwarf the benefits of increased topographic resolution. For example, most existing inundation maps in California were produced at a resolution ranging from 75 to 250 m. Nonetheless, we performed full-inundation computations to avoid the well-known underestimation issues that plague threshold models, which stop the calculation at some offshore depth (Synolakis and Bernard, 2006).

We considered 9 m as a minimum for run-up, about 300 m inland in Palaikastro, which corresponds to the deposits in Buildings 6 and 7. We also constrained the inverse model by requiring at least 5 m inundation in Amnissos – a conservative estimate. We then performed a series of over 50 simulations to infer the size of the initial wave during the eruption, assuming that the initial wave was generated by pyroclastic flows, which we model as sub-aerial landslides (Synolakis et al., 2002). The largest wave would have the impact that presents itself in the stratigraphic evidence we described for the coastal Promontory and East Beach hillocks.

Our results suggest that the initial wave was two to four times the size of the wave that had been inferred earlier on the basis of the available evidence before our work. The initial wave that best fits the stratigraphic data is a wave with +35 to −15 m initial amplitude at the generation region with a crest length of about 15 km. This size of wave is consistent with recent findings of massive pyroclastic flow deposits around Santorini (Sigurdsson et al., 2006), which suggest that the total volume of ejecta was about twice the size of earlier estimations.

For comparison, the tsunami that devastated the north coast of Papua New Guinea in 1998 was triggered by a large underwater landslide. Detailed modeling, based upon existing data concerning source and run-up, yielded results suggesting an initial wave of +15 to −8 m at generation (Synolakis et al., 2002). The tsunami resulted in 12 m flow depths at Sissano, Papua New Guinea, killing more than 2100 people. The generation of tsunamis by submarine mass failure can be considered partially analogous to pyroclastic flows slumping into the water.

Our results from Palaikastro for a tsunami generated during the Minoan Santorini eruption appear consistent with the 1956 Amorgos tsunami, the largest tsunami event in the 20th century in the Eastern Mediterranean. The latter tsunami was triggered by submarine slumping into a trench near the island of Amorgos (Fig. 1), caused by an earthquake ($Ms = 7.8$). Eye witness accounts and measurements (Okal et al., 2004) suggest a 22 m run-up near the epicenter in Amorgos, 2 m run-up near Amnissos (Crete), and, according to our information, 4 m run-up in Palaikastro. The source region of the 1956 tsunami lies rather close to Santorini from the perspective of Palaikastro (Fig. 1). Based upon the above Amorgos tsunami data, one would infer substantial impact in Palaikastro from the Minoan Santorini eruption, even without a detailed numerical model and without accounting for directivity effects that are anyway hard to quantify for pyroclastic flows.

9. Discussion and conclusions

All six described field sections along the coastal cliff at the Promontory and East Beach hillocks were shown to have a number of sedimentary features that match tsunami signatures (Dominey-Howes, 2004; Dominey-Howes et al., 2006: Scheffers and Kelletat, 2004):

(1) Sharp basal contact with the underlying sediment in the four field sections along the East Beach cliff – the distinct boundary with the hard basal conglomerate at the Promontory is obvious.
(2) Intraclasts of volcanic Santorini ash in the lower part of field section 2 at the Promontory.
(3) Reworked material – building stones – in the lower part of the geoarchaeological layer in field section 4 at the East Beach.
(4) Presence of individual marine shells in the geoarchaeological layer at both the Promontory and East Beach.
(5) Marine micro-fauna of coralline algae and foraminifera, as well as inter-tidal beach-rock and rounded sand grains, present in thin sections from samples of sediment in the upper remaining part of the 'staircase' building, below an apparent stepping stone and above the upper remaining

stone of the western wall – field section 1 at the Promontory.

(6) Imbrication of ceramic sherds, building debris, bones and/or rounded pebbles in field section 1 at the Promontory and field section 3 at the East Beach cliff.

(7) The geoarchaeological layer shows in all field sections at the Promontory and East Beach a multi-modal, non-sorted, chaotic particle size composition that includes fine red-dish-brown silt to clay size sediment, sand, gravel, rounded pebbles, building stones, ceramic sherds and cups.

Many of these features cannot be explained in terms of "normal" archaeological formation processes (Schiffer, 1987), but do fit tsunami signatures, as described above. The marine shells occur singularly and occasionally in a random distribution pattern and not as clusters. Hence their presence cannot be explained in terms of food middens. Stream channel deposition from the hinterland can be safely excluded to explain rounded pebbles and imbrication in view of the isolated geomorphological position of the Promontory and East beach hillocks. It seems that the Bronze Age buildings or building remains at these hillocks both influenced tsunami deposition patterns and helped to preserve debris from eroding during tsunami backwash and in later periods.

Considering the highest elevation of these deposits on the East Beach cliff and the lower sea level in Minoan times, the tsunami wave(s) must have been at least 9 m high, but probably considerably higher to reach the buildings on these elevated parts with sufficient destruction force. The backwash seaward flow was probably somewhat less powerful on the Promontory and East Beach hillocks, as compared to the lower parts of the coastline.

The observed and described features of geoarchaeological deposits in the field sections along the Promontory and East Beach cliffs do not fit storm sedimentation, except perhaps for some marine shells – not *in situ* – at the lower Promontory. The distinction between sea storm and tsunami deposits has been precisely and eloquently described by Morton et al. (2007) in relation to the differences in hydrodynamics and sediment-sorting processes during transport: "Tsunami deposition results from a few high-velocity, long-period waves that entrain sediment from the shoreface, beach, and landward erosion zone. Tsunamis can have flow depths greater than 10 m, transport sediment primarily in suspension, and distribute the load over a broad region where sediment falls out of suspension when flow decelerates. In contrast, storm inundation generally is gradual and prolonged, consisting of many waves that erode beaches and dunes with no significant overland return flow until after the main flooding" (Morton et al., 2007, p. 184). The authors noted that storm flow depths are commonly less than 3 m, while "sediment is transported primarily as bed load by traction, and the load is deposited within a zone relatively close to the beach" (Morton et al., 2007, p. 184). The multi-modal chaotic composition and rather similar appearance of the geoarchaeological layer over a wide area along the Promontory and East Beach cliffs, albeit with local variations as described in the field sections, do fit tsunami but not storm deposition.

Airborne volcanic ash was already present at the Promontory area, when it was reworked by short-lived tsunami action that did neither result in total removal nor in homogeneous mixing. Volcanic ash intraclasts became deposited with red-dish-brown fine sediment and coarse material in the lower part of the geoarchaeological deposit in section 2 of the Promontory. Micromorphology studies showed that volcanic ash particles also occur in low concentration in the redeposited fine red-brown sediment. Short-lived tsunami action did not lead to sorting of particle sizes and distinct layering, but to rather sudden dump deposits, mixing various constituents together.

The tsunami appeared to have occurred during the Minoan Santorini eruption, possibly in the third or fourth eruption phase, but *after* the deposition of airborne volcanic ash over eastern Crete. Geological, archaeological and radiocarbon criteria date the geoarchaeological deposits, containing volcanic Santorini ash, to the time of the Minoan eruption. The two dated cattle bones covered by pottery sherds – all imbricated – seem to be food remains from the destroyed coastal houses, perhaps the last meal, before the tsunami struck. It seems that both the broken dishes and the bones were deposited together by strong currents, causing contact imbrication of flat and elongated objects. Indeed, pottery sherds and other flat settlement debris are well suited, due to their shape, to obtain imbrication patterns in case of tsunami action. An earthquake could not have caused such imbrication (Figs. 7, 11). Recognition of geoarchaeological tsunami signatures is a new field that needs to be developed.

The initial results of inverse tsunami modeling, based on the new field evidence, suggest a wave of +35 to −15 m initial amplitude and a crest length of about 15 km in the Santorini generation region. That is powerful for a tsunami. For example the 1998 Papua New Guinea tsunami, which had an initial wave of +15 to −8 m at generation, roughly half the above dimensions, caused catastrophic flow depths of 12 m at Sissano.

The tsunami waves at Palaikastro apparently inundated the Minoan town completely, which would explain many puzzling LM IA deposits encountered during previous excavations (MacGillivray et al., 1987, 1991, 1992, 1998). We have noted similar evidence at other Minoan sites, for example at Malia, where the palace ceased to function in LM IA. Chaotic deposits, including admixtures of LM IA pottery and pumice, analogous in terms of sedimentation fabric to those at Palaikastro, are visible along coastal cliffs near Malia (see Blackman, 2000, for description of the coast).

But the tsunami did not cause the end of the Minoan civilization. There was a building boom characterized by fine masonry during the subsequent LM IB period. Nevertheless, the Santorini eruption and accompanying tsunami seem to have triggered the beginning of the end for the Minoans, whose major population centres were un-walled and largely situated along the coastline, and whose naval defence was probably devastated. Invasion and destruction followed in LM IB. The gradual rebuilding and repopulation of Crete in the subsequent

LM II and LM IIIA periods were controlled by a military-minded authority that converted the Minoan Linear A script to suite the Greek language. This leaves little doubt that the invaders were Greeks from the mainland, Mycenae in particular, whose navy harboured in the protected Corinthian gulf.

A gradual invasion of Crete from west to east would explain the differences in archaeomagnetic and radiocarbon dates from LM IB burnt destruction deposits (Tarling and Downey, 1990) and why these destructions in the east were contemporary with central Cretan LM II (MacGillivray, 1997).

Acknowledgements

We are most grateful to the late N. Papadakis, Director of Antiquities for Eastern Crete, and the Greek Ministry of Culture, for their permission and constant support of our research, which was partly funded by the Institute for Aegean Prehistory. We thank the Stichting Midbar Foundation for financial support of the micromorphology and volcanic ash studies. Our research was undertaken under the auspices of the geological and geomorphological survey of the Palaikastro Excavations of the British School at Athens and under the auspices of the Institute of Geological and Mineral Exploration (IGME, Greece) to sample coastal sediments throughout Crete as part of the Aegean Tsunamis Research Programme. We thank J. Moody for discussions in the field that strengthened our tsunamigenic interpretations. We thank K. Linse for identifying photographed marine shells. The logistical support and help of the British Excavations at Palaikastro are acknowledged, though the authors alone are responsible for both the research and conclusions. The reviewers comments considerably improved the final text and lay-out of the article.

References

Aerts-Bijma, A.T., van der Plicht, J., Meijer, H.A.J., 2001. Automatic AMS sample combustion and CO_2 collection. Radiocarbon 43, 293–298.

Ambraseys, N.N., 1960. The seismic sea wave of July 9, 1956, in the Greek Archipelago. Journal of Geophysical Research 65, 1257–1265.

Antonopoulos, J., 1992. The great Minoan eruption of Thera volcano and the ensuing tsunami in the Greek Archipelago. Natural Hazards 5, 153–168.

Betancourt, P.P., Goldberg, P., Hope Simpson, R., Vitaliano, C.J., 1990. Excavations at Pseira: the evidence for the Theran eruption. In: Hardy, D.A., Renfrew, A.C. (Eds.), Thera and the Aegean World III, vol. 3. The Thera Foundation, London, pp. 96–99.

Bietak, M., 2003. Science versus archaeology: problems and consequences of High Aegean Chronology. In: Bietak, M. (Ed.), The Synchronisation of Civilisations in the Eastern Mediterranean in the Second Millennium B.C. – II, pp. 23–33.

Bietak, M., Höflmayer, F., 2007. Introduction: high and low chronology. In: Bietak, M., Czerny, E. (Eds.), The Synchronisation of Civilisations in the Eastern Mediterranean in the Second Millennium B.C. – III. Austrian Academy of Sciences, Vienna, pp. 13–23.

Blackman, D., 2000. Archaeology in Greece 1999–2000. Archaeological Reports 1999–2000. British School at Athens, London.

Bond, A., Sparks, R.S.J., 1976. The Minoan eruption of Santorini, Greece. Journal of the Geological Society of London 132, 1–16.

Bronk Ramsey, C., Manning, S.W., Galimberti, M., 2004. Dating the volcanic eruption at Thera. Radiocarbon 46, 325.

Bruins, H.J., 2007. Charcoal radiocarbon dates of Tell el-Dab'a. In: Bietak, M., Czerny, E. (Eds.), The Synchronisation of Civilisations in the Eastern Mediterranean in the Second Millennium B.C. – III. Austrian Academy of Sciences, Vienna, pp. 65–77.

Bruins, H.J., Mook, W.G., 1989. The need for a calibrated radiocarbon chronology of Near Eastern Archaeology. Radiocarbon 31 (3), 1019–1029.

Bruins, H.J., Van der Plicht, J., 2003. Assorting and synchronising archaeological and geological strata with radiocarbon: the Southern Levant in relation to Egypt and Thera. In: Bietak, M. (Ed.), The Synchronisation of Civilizations in the Eastern Mediterranean in the 2nd Millennium BC – II. Austrian Academy of Sciences, Vienna, pp. 35–42.

Bruins, H.J., Van der Plicht, J., Mazar, A., 2003. ^{14}C dates from Tel Rehov: Iron-Age chronology, Pharaohs and Hebrew Kings. Science 300 (5617), 315–318.

Bryant, E., 2001. Tsunami – The Underrated Hazard. Cambridge University Press, Cambridge.

Carey, S., Morelli, D., Sigurdsson, H., Bronto, S., 2001. Tsunami deposits from major explosive eruptions: an example from the 1883 eruption of Krakatau. Geology 29 (4), 347–350.

Cioni, R., Gurioli, L., Sbrana, A., Vougioukalakis, G., 2000. Precursory phenomena and destructive events related to the Late Bronze Age Minoan (Thera, Greece) and AD 79 (Vesuvius, Italy) Plinian eruptions; inferences from the stratigraphy in the archaeological areas. In: McGuire, W.G., Griffiths, D.R., Hancock, P.L., Stewart, I.S. (Eds.), The Archaeology of Geological Catastrophes. Special Publication 171. Geological Society, London, pp. 123–141.

Cita, M.B., Camerlenghi, A., Kastens, K.A., McCoy, F.W., 1984. New findings of Bronze Age homogenites in the Ionian Sea: geodynamic implications for the Mediterranean. Marine Geology 55, 47–62.

Courty, M.A., Goldberg, P., Macphail, R., 1989. Soils and Micromorphology in Archaeology. Cambridge University Press, Cambridge.

Dawson, A.G., Shi, S., 2000. Tsunami deposits. Pure and Applied Geophysics 157, 875–897.

Dominey-Howes, D.T.M., 2004. A re-analysis of the Late Bronze Age eruption and tsunami of Santorini, Greece, and the implications for the volcano-tsunami hazard. Journal of Volcanology and Geothermal Research 130, 107–132.

Dominey-Howes, D.T.M., Cundy, A.B., Croudace, I., 2000. High energy marine flood deposits on Astypalaea Island, Greece: possible evidence for the AD 1956 southern Aegean tsunami. Marine Geology 163, 303–315.

Dominey-Howes, D.T.M., Humphreys, G.S., Hesse, P.P., 2006. Tsunami and palaeotsunami depositional signatures and their potential value in understanding the late-Holocene tsunami record. The Holocene 16 (8), 1095–1107.

Doumas, C.G., 1983. Thera: Pompeii of the ancient Aegean. Thames and Hudson, London.

Doumas, C., Papazoglou, L., 1980. Santorini tephra from Rhodes. Nature 287, 322–324.

Driessen, J., Macdonald, C.F., 1997. The Troubled Island, Minoan Crete before and after the Santorini eruption. In: Aegaeum 17. Université de Liège/University of Texas, Liège/Austin.

Driessen, J., Macdonald, C.F., 2000. The eruption of the Santorini volcano and its effect on Minoan Crete. In: McGuire, W.G., Griffiths, D.R., Hancock, P.L., Stewart, I.S. (Eds.), The Archaeology of Geological Catastrophes. Special Publication 171. Geological Society, London, pp. 81–93.

Druitt, T.H., Edwards, L., Mellors, R.M., Pyle, D.M., Sparks, R.S.J., Lanphere, M., Davies, M., Barreiro, B., 1999. Santorini Volcano. Geological Society, London (Special Memoir, 19).

Eastwood, W.J., Pearce, N.J.G., Westgate, J.A., Perkins, W.T., 1998. Recognition of Santorini (Minoan) tephra in lake sediments from Gölhisar Gölü, southwest Turkey, by laser ablation ICP-MS. Journal of Archaeological Science 25, 677–687.

Eastwood, W.J., Pearce, N.J.G., Westgate, J.A., Perkins, W.T., Lamb, H.F., Roberts, N., 1999. Geochemistry of Santorini tephra in lake sediments from Southwest Turkey. Global and Planetary Change 21, 17–29.

Flemming, N.C., Webb, C.O., 1986. Tectonic and eustatic coastal changes during the last 10,000 years derived from archaeological data. Zeitschrift für Geomorphologie 62, 1–29.

Friedrich, W.L., 2000. Fire in the Sea: The Santorini Volcano. Cambridge University Press, Cambridge.

Friedrich, W.L., Kromer, B., Friedrich, M., Heinemeier, J., Pfeiffer, T., Talamo, S., 2006. Santorini eruption radiocarbon dated to 1627–1600 B.C. Science 312, 548.

Galanopoulos, A.G., 1960. Tsunamis observed on the coasts of Greece from antiquity to present time. Annali di Geofisica 13, 369–386.

Goff, J., Liu, P.L.F., Higman, B., Morton, R., Jaffe, B.E., Fernando, H., Lynett, P., Fritz, H., Synolakis, C., Fernando, S., 2006. Sri Lanka field survey after the December 2004 Indian Ocean tsunami. Earthquake Spectra 22 (3), 155–172.

Gelfenbaum, G., Jaffe, B., 2003. Erosion and sedimentation from the 17 July, 1998 Papua New Guinea Tsunami. Pure Applied Geophysics 160, 1969–1999.

Heiken, G.H., McCoy, F.W., 1984. Caldera development during the Minoan eruption, Thera, Cyclades, Greece. Journal of Geophysical Research 89, 8441–8462.

Heiken, G.H., McCoy, F.W., 1990. Precursory activity to the Minoan eruption, Thera, Greece. In: Hardy, D.A., Renfrew, A.C. (Eds.), Thera and the Aegean World III, vol. 2. The Thera Foundation, London, pp. 79–88.

Inbar, M., Ostera, H.A., Parica, C.A., Remesal, M.B., Salani, F.M., 1995. Environmental assessment of 1991 Hudson volcano eruption ashfall effects on southern Patagonia region, Argentina. Environmental Geology 25 (2), 119–125.

Jaffe, B.E., Gelfenbaum, G., 2002. Using tsunami deposits to improve assessment of tsunami risk. In: Conference Proceedings Solutions to Coastal Disasters. Coasts, Oceans, Ports, and Rivers Institute (COPRI) of the American Society of Civil Engineers, pp. 836–847.

Jaffe, B.E., Borrero, J.C., Prasetya, G.S., Peters, R., McAdoo, B., Gelfenbaum, G., Morton, R., Ruggiero, P., Higman, B., Dengler, L., Hidayat, R., Kingsley, E., Kongko, W., LukijantoMoore, A., Titov, V., Yulianto, E., 2006. Northwest Sumatra and offshore islands field survey after the December 2004 Indian Ocean tsunami. Earthquake Spectra 22 (S3), S105–S135.

Jarosewich, E., Nelen, J.A., Norberg, J.A., 1980. Reference samples for electron microprobe analysis. Geostandards Newsletter 4, 43–47.

Johansson, C.E., 1976. Structural studies of frictional sediments. Geografiska Annaler. Series A. Physical Geography 58 (4), 201–301.

Jochum, K.P., Dingwell, D.B., Rocholl, A., Stoll, B., Hofmann, A.W., et al., 2000. The preparation and preliminary characterization of eight geological MPI-DING reference glasses for in-situ microanalysis. Geostandards Newsletter 24, 87–133.

Kayan, I., 1988. Late Holocene sea-level changes on the western Anatolian coast. Palaeogeography, Palaeoclimatology, Palaeoecology 68, 205–218.

Kayan, I., 1991. Holocene geomorphic evolution of the Beşik plain and changing environment of ancient man. Studia Troica 1, 79–92.

Keller, J., 1980a. Did the Santorini eruption destroy the Minoan world? Nature 287, 779.

Keller, J., 1980b. Prehistoric pumice tephra on Aegean islands. In: Doumas, C. (Ed.), Thera and the Aegean World, vol. II. Thera Foundation, London, pp. 49–56.

Keller, J., Ryan, W.B.F., Ninkovich, D., Altherr, R., 1978. Explosive volcanic activity in the Mediterranean over the past 200,000 yr as recorded in deep-sea sediments. Geological Society of America Bulletin 89, 591–604.

Keller, J., Rehren, Th., Stadlbauer, E., 1990. Explosive volcanism in the Hellenic Arc: a summary and review. In: Hardy, D., Keller, J., Galanopoulos, V.P., Flemming, N.C., Druitt, T.H. (Eds.), Thera and the Aegean World III, vol. 2. The Thera Foundation, London, pp. 13–26.

Liu, P.L.F., Lynett, P., Fernando, H., Jaffe, B.E., Fritz, H., Higman, B., Morton, R., Goff, J., Synolakis, C., 2005. Observations by the International Tsunami Survey Team in Sri Lanka. Science 308, 1595.

MacGillivray, J.A., 1997. The re-occupation of Eastern Crete in the Late Minoan II–IIIA1/2 periods. In: Driessen, J., Farnoux, A. (Eds.), La Crète Mycénienne, (BCH Suppl. 30). École Française D'Athènes, Paris, pp. 275–279.

MacGillivray, J.A., Sackett, L.H., Smyth, D., 1984. An archaeological survey of the Roussolakos area at Palaikastro. The Annual of the British School of Archaeology at Athens 79, 129–141 (Plates 8–13).

MacGillivray, J.A., Sackett, L.H., Driessen, J., Smyth, D., 1987. Excavations at Palaikastro 1986. The Annual of the British School of Archaeology at Athens 82, 135–154 (Plates 19–24).

MacGillivray, J.A., Sackett, L.H., Driessen, J., Smyth, D., 1991. Excavations at Palaikastro 1990. The Annual of the British School of Archaeology at Athens 86, 121–147 (Plates 6–16).

MacGillivray, J.A., Sackett, L.H., Driessen, J., Farnoux, A., Smyth, D., 1992. Excavations at Palaikastro 1991. The Annual of the British School of Archaeology at Athens 87, 121–152 (Plates 3–7).

MacGillivray, J.A., Sackett, L.H., Driessen, J., Hemingway, S., 1998. Excavations at Palaikastro 1994 and 1996. The Annual of the British School of Archaeology at Athens 93, 221–268 (Plates 38–50).

Maheshwari, B.K., Sharma, M.L., Narayan, J.P., 2006. Geotechnical and structural damage in Tamil Nadu, India, from the December 2004 Indian Ocean tsunami. Earthquake Spectra 22 (3), 475–493.

Manning, S.W., 1999. A Test of Time – The Volcano of Thera and The Chronology and History of the Aegean and East Mediterranean in the Mid Second Millennium BC. Oxbow Books, Oxford.

Manning, S.W., Bronk Ramsay, C., Kutschera, W., Higham, T., Kromer, B., Steier, P., Wild, E.M., 2006. Chronology for the Aegean Late Bronze Age 1700–1400 B.C. Science 312, 565–569.

Marinatos, S., 1939. The volcanic destruction of Minoan Crete. Antiquity 13, 425–439.

McCoy, F.W., 1980. The upper Thera (Minoan) ash in deep-sea sediments: distribution and comparison with other ash layers. In: Doumas, C. (Ed.), Thera and the Aegean World, vol. II. Thera Foundation, London, pp. 49–56.

McCoy, F.W., Heiken, G., 2000. Tsunami generated by the Late Bronze Age eruption of Thera (Santorini), Greece. Pure and Applied Geophysics 157, 1227–1256.

McCoy, F.W., Synolakis, C.E., Papadopoulous, G.A., 2000. Tsunami generated during the LBA eruption of Thera – evidence from modeling and tsunami deposits. Bulletin of the American Geophysical Union 81 (48) (San Francisco, California).

McCoy, F.W., Dunn, S., 2002. Modelling the climatic effects of the LBA eruption of Thera: new calculations of tephra volumes may suggest a significantly larger eruption than previously reported (abstract). In: Proceedings of the Chapman Conference on Volcanism and the Earth's Atmosphere. American Geophysical Union, Santorini, Greece, pp. 21–22.

McFadgen, B.G., Goff, J.R., 2007. Tsunamis in the New Zealand archaeological record. Sedimentary Geology 200, 263–274.

Minoura, K., Imamura, F., Kuran, U., Nakamura, T., Papadopoulos, G.A., Takahashi, T., Yalciner, A.C., 2000. Discovery of Minoan tsunami deposits. Geology 28, 59–62.

Moore, A., Nishimura, Y., Gelfenbaum, G., Kamataki, T., Triyono, R., 2006. Sedimentary deposits of the 26 December 2004 tsunami on the northwest coast of Aceh, Indonesia. Earth Planets Space 58 (2), 253–258.

Morton, R.A., Gelfenbaum, G., Jaffe, B.E., 2007. Physical criteria for distinguishing sandy tsunami and storm deposits using modern examples. Sedimentary Geology 200, 184–207.

Nanayama, F., Satake, K., Shimokawa, K., Shigeno, K., Miyasaka, S., 1998. Sedimentary characteristics of tsunami deposits: examples from the 1993 Hokkaido Nansei-oki tsunami, Northern Japan. Western Pacific Geophysics Meeting. American Geophysical Union (abstract).

Nanayama, F., Shigeno, K., Satake, K., Shimokawa, K., Koitabashi, S., Miyasaka, S., Ishii, M., 2000. Sedimentary differences between the 1993 Hokkaido-nansei-oki tsunami and the 1959 Miyakojima typhoon at Taisei, southwestern Hokkaido, northern Japan. Sedimentary Geology 135 (1), 255–264.

Nomanbhoy, N., Satake, K., 1995. Generation mechanism of tsunamis from the 1883 Krakatau eruption. Geophysical Research Letters 22 (4), 509–512.

Okal, E.A., Synolakis, C.E., Yalciner, A.C., 2004. The Amorgos, Greece Earthquake and Tsunami of 09 July 1956: Focal Mechanism and Field Survey. American Geophysical Union, San Francisco, California (Fall Meeting, Session OS23D–1358).

Papastamatiou, I., 1959. Geological Map of Crete, Map Sheet 23, Sitia. Geological Survey and Geographical Service of the Greek Army, Athens.

Pareschi, M.T., Favalli, M., Boschi, E., 2006. Impact of the Minoan tsunami of Santorini: simulated scenarios in the eastern Mediterranean. Geophysical Research Letters 33 (18), L18607.

Pearce, N.J.G., Eastwood, W.J., Westgate, J.A., Perkins, W.T., 2002. Trace element composition of single glass shards in distal Minoan tephra from SW Turkey. Journal of Geological Society 159, 545–556.

Perissoratis, C., Papadopoulos, G., 1999. Sediment instability and slumping in the southern Aegean Sea and the case history of the 1956 tsunami. Marine Geology 161, 287–305.

Reinhardt, E.G., Goodman, B.N., Boyce, J.I., Lopez, G., van Hengstum, P., Rink, W.J., Mart, Y., Raban, A., 2006. The tsunami of 13 Decemebr A.D. 115 and the destruction of Herod the Great's harbor at Ceasarea Maritima, Israel. Geology 34 (12), 1061–1064.

Scheffers, A., 2004. Tsunami imprints on the Leeward Netherlands Antilles (Aruba, Curaçao, Bonaire) and their relation to other coastal problems. Quaternary International 120, 163–172.

Scheffers, A., Kelletat, D., 2003. Sedimentological and geomorphologic tsunami imprints worldwide – a review. Earth Science Reviews 63, 83–92.

Scheffers, A., Kelletat, D., 2004. Bimodal tsunami deposits – a neglected feature in paleo-tsunami research. Coastline Reports 1, 67–75.

Schiffer, M.B., 1987. Formation Processes of the Archaeological Record. University of New Mexico Press, Albuquerque.

Siani, G., Paterne, M., Michel, E., Sulpizio, R., Sbrana, A., Arnold, M., Haddad, G., 2001. Mediterranean Sea surface radiocarbon reservoir age changes since the last glacial maximum. Science 294, 1917–1920.

Sigurdsson, H., Carey, S., 1989. Plinian and coignimbrite tephra fall from the 1815 eruption of Tambora volcano. Bulletin of Volcanology 51, 243–270.

Sigurdsson, H., Carey, S., Alexandri, M., Vougioukalakis, G., Croff, K., Roman, C., Sakellariou, D., Anagnostou, C., Rousakis, G., Ioakim, C., Gogou, A., Ballas, D., Misaridis, T., Nomikou, P., 2006. Marine investigations of Greece's Santorini volcanic field. EOS, Transactions American Geophysical Union 87 (24), 337–342.

Simkin, T., Fiske, R.S., 1983. Krakatau 1883: the volcanic eruption and its effects. Smithsonian Institution Press, Washington, D.C.

Smith, D., 2005. Tsunami: a research perspective. Geology Today 21, 64–68.

Sneh, Y., Klein, M., 1984. Holocene sea level changes at the coast of Dor, southeast Mediterranean. Science 226 (4676), 831–832.

Soles, J.S., Davaras, C., 1990. Theran Ash in Minoan Crete: New Excavations on Mochlos. In: Hardy, D.A., Renfrew, A.C. (Eds.), Thera and the Aegean World III, vol. 3. The Thera Foundation, London, pp. 89–95.

Sparks, R.S.J., Wilson, C.J.N., 1990. The Minoan deposits: a review of their characteristics and interpretation. In: Hardy, D., Keller, J., Galanopoulos, V.P., Flemming, N.C., Druitt, T.H. (Eds.), Thera and the Aegean World III, vol. 2. The Thera Foundation, London, pp. 89–99.

Synolakis, C.E., Bardet, J.P., Borrero, J.C., Davies, H.L., Okal, E.A., Silver, E.A., Sweet, S., Tappin, D.R., 2002. The slump origin of the 1998 Papua New Guinea Tsunami. Proceedings of the Royal Society A: Mathematical, Physical and Engineering Sciences 458, 763–769.

Synolakis, C.E., Kong, L., 2006. Runup measurements of the December 2004 Indian Ocean tsunami. Earthquake Spectra 22 (3), 67–91.

Synolakis, C.E., Bernard, E.N., 2006. Tsunami science before and beyond Boxing Day 2004. Philosophical Transactions of the Royal Society A: Mathematical, Physical and Engineering Sciences 364 (1845), 2231–2265.

Tarling, D.H., Downey, W.S., 1990. Archaeomagnetic results from Late Minoan destruction levels on Crete and the 'Minoan' tephra on Thera. In: Hardy, D.A., Renfrew, A.C. (Eds.), Thera and the Aegean World III, vol. 3. The Thera Foundation, London, pp. 146–159.

Thorarinsson, S., 1978. Some comments on the Minoan eruption of Santorini. In: Doumas, C. (Ed.), Thera and The Aegean World I, Part One: Geosciences. Thera and the Aegean World, London, pp. 263–275.

Titov, V., Synolakis, C.E., 1998. Numerical modeling of tidal wave runup. Journal of Waterway, Port, Coastal and Ocean Engineering 124 (4), 157–171.

Todd, S.P., 1996. Process deduction from fluvial sedimentary structures. In: Carling, P.A., Dawson, M.R. (Eds.), Advances in Fluvial Dynamics and Stratigraphy. Wiley, Chichester, pp. 299–350.

Van der Plicht, J., Bruins, H.J., 2001. Radiocarbon dating in Near-Eastern contexts: confusion and quality control. Radiocarbon 43 (3), 1155–1166.

Van der Plicht, J., Wijma, S., Aerts, A.T., Pertuisot, M.H., Meijer, H.A.J., 2000. The Groningen AMS facility: status report. Nuclear Instruments and Methods B172, 58–65.

Vitaliano, C.J., Vitaliano, D.B., 1974. Volcanic tephra on Crete. American Journal of Archaeology 78, 19–24.

Warren, P., Hankey, V., 1989. Aegean Bronze Age Chronology. Bristol Classical, Bristol.

Watkins, N.D., Sparks, R.S.J., Sigurdsson, H., Huang, T.C., Federman, A., Carey, S., Ninkovich, D., 1978. Volume and extent of the Minoan tephra from Santorini Volcano: new evidence from deep-sea sediment cores. Nature 271, 122–126.

Wiener, M.H., 2003. Time out: the current impasse in Bronze Age archaeological dating. In: Foster, K.P., Laffineur, R. (Eds.), METRON: Measuring The Aegean Bronze Age. Aegaeum 24. Université de Liège/University of Texas, Liège/Austin, pp. 363–399.

Wiener, M.H., 2007. Times change: the current state of the debate in Old World chronology. In: Bietak, M., Czerny, E. (Eds.), The Synchronisation of Civilisations in the Eastern Mediterranean in the Second Millennium B.C. – III. Austrian Academy of Sciences, Vienna, pp. 25–47.

Wilson, L., 1972. Explosive volcanic eruptions – II. The atmosphere trajectories of pyroclasts. Geophysical Journal of the Royal Astronomical Society 30, 381–392.

Yokoyama, I., 1978. The tsunami caused by the prehistoric eruption of Thera. In: Doumas, C. (Ed.), Thera and the Aegean World I, Part One: Geosciences. Thera and The Aegean World, London, pp. 277–283.